ECONOMIC GEOLOGY RESEARCH INSTITUTE

University of the Witwatersrand
Johannesburg

GEOLOGY AND GEODYNAMIC SETTING OF ARCHAEAN SILICIC METAVOLCANICLASTIC ROCKS OF THE BIEN VENUE FORMATION, FIG TREE GROUP, NORTHEAST BARBERTON GREENSTONE BELT, SOUTH AFRICA

E. A. KOHLER and C. R. ANHAEUSSER

INFORMATION CIRCULAR No. 348

UNIVERSITY OF THE WITWATERSRAND
JOHANNESBURG

GEOLOGY AND GEODYNAMIC SETTING OF ARCHAEAN SILICIC METAVOLCANICLASTIC ROCKS OF THE BIEN VENUE FORMATION, FIG TREE GROUP, NORTHEAST BARBERTON GREENSTONE BELT, SOUTH AFRICA

by

E.A. KOHLER[1,2] and C.R. ANHAEUSSER[2]

([1]Council for Geoscience, Geological Survey of South Africa, P/Bag X112, Pretoria, 0001 Republic of South Africa; [2]Economic Geology Research Institute, University of the Witwatersrand, P/Bag 3, WITS 2050, Johannesburg, Republic of South Africa;

[1] Present address: Normandy Mining Limited, PO Box 1652, Subiaco, Western Australia 6904, Australia. Corresponding author. Fax: +61-8-9450-5331
E-mail addresses: [1]ernstk@smartchat.net.au ; [2] 065cra@cosmos.wits.ac.za)

ECONOMIC GEOLOGY RESEARCH INSTITUTE
INFORMATION CIRCULAR No. 348

September, 2000

GEOLOGY AND GEODYNAMIC SETTING OF ARCHAEAN SILICIC METAVOLCANICLASTIC ROCKS OF THE BIEN VENUE FORMATION, FIG TREE GROUP, NORTHEAST BARBERTON GREENSTONE BELT, SOUTH AFRICA

ABSTRACT

Mapping of the northeastern part of the Barberton greenstone belt (BGB) has delineated a new lithostratigraphic unit, the Bien Venue Formation, within the Fig Tree Group, Swaziland Supergroup, South Africa. The new formation has been previously dated at 3256 ± 1 Ma and 3259 ± 5 Ma, and is composed mainly of siliceous and aluminous quartz-muscovite (± andalusite ± chlorite ± chloritoid ± pyrophyllite) schists derived from a proximal sequence of calc-alkaline, quartz-phyric, dacitic-to-rhyodacitic volcaniclastic protoliths. Subordinate rock types include banded chert, biotite-plagioclase (± chlorite ± carbonate) schists derived from plagioclase-phyric calc-alkaline dacitic volcaniclastic assemblages, and chlorite (± carbonate ± amphibole) schists representing altered basalt or basalt-andesite with a transitional tholeiitic - calc-alkaline signature. These rocks were deposited on deep-water shales, turbiditic greywackes, banded iron-formations and silicic metavolcaniclastic assemblages correlated with the Belvue Road Formation, and are, in turn, overlain by alluvial to shallow-marine sandstones and conglomerates of the Moodies Group along a regional unconformity. In places, the quartz-muscovite schists host subeconomic base metal and barite deposits of probable volcanogenic origin. These deposits suggest that the depositional environment of the Bien Venue strata was largely subaqueous, but may have varied from deep (>1 km depth) to shallow water.

The Bien Venue rocks were previously included in the Theespruit Formation of the Onverwacht Group. However, available isotopic age data now indicate that they are some 290 Ma younger than the oldest assemblages within the lower Onverwacht. The schists are also 30 Ma older than plagioclase-phyric dacitic rocks within the Schoongezicht Formation (ca 3226 Ma), the uppermost formation of the Fig Tree Group along the northwest flank of the BGB, precluding direct correlation with this unit. Published ages suggest that the Bien Venue Formation is a temporal correlative of proximal volcaniclastic rocks making up the Auber Villiers Formation (3256 Ma), and possibly also some distal dacitic tuffaceous sequences within the Mapepe Formation (3258 to 3227 Ma), both of which form part of the southern Fig Tree facies.

The protoliths of the Bien Venue schists were geochemically similar to Phanerozoic mature active continental margin suites. Variably fractionated rare earth element profiles, moderate abundances of Yb and Y, and relative depletions of Ta-Nb, P and Ti on normalized immobile multi-element diagrams, are consistent with hydrous fusion of upper mantle material above steeply subducted oceanic crust undergoing dehydration. The features suggest that the Bien Venue Formation records Early Archaean continental arc volcanism along the northeast flank of what is now the BGB.

oOo

GEOLOGY AND GEODYNAMIC SETTING OF ARCHAEAN SILICIC METAVOLCANICLASTIC ROCKS OF THE BIEN VENUE FORMATION, FIG TREE GROUP, NORTHEAST BARBERTON GREENSTONE BELT, SOUTH AFRICA

CONTENTS

__________oOo__________

Published by the Economic Geology Research Institute
Department of Geology
University of the Witwatersrand
1 Jan Smuts Avenue
Johannesburg 2001

www.wits.ac.za/egru

ISBN 1-86838-292-3

GEOLOGY AND GEODYNAMIC SETTING OF ARCHAEAN SILICIC METAVOLCANICLASTIC ROCKS OF THE BIEN VENUE FORMATION, FIG TREE GROUP, NORTHEAST BARBERTON GREENSTONE BELT, SOUTH AFRICA

INTRODUCTION

The 160 x 50 km Barberton greenstone belt (BGB), located along the southeast margin of the Kaapvaal Craton, southern Africa, is a well-preserved inlier of metamorphosed and deformed Archaean volcano-sedimentary lithologies (Fig. 1). Most of the important insights into the evolution of the BGB followed the pioneering regional mapping programmes of Hall (1918), Visser (1956), Viljoen, M.J. and Viljoen (1969a,b), and Viljoen, R.P and Viljoen, (1969a) who provided the first stratigraphic classifications of the Swaziland Supergroup (Anhaeusser, 1973; Lowe and Byerly, 1999), also referred to as the Barberton Sequence (SACS, 1980). These studies defined three major stratigraphic units on the basis of dominant rock types, referred to from the base upwards as the Onverwacht, Fig Tree and Moodies Groups.

Numerous structural, petrological and isotopic studies since then have provided comprehensive, though often controversial, accounts of the stratigraphy of these groups. However, most of this work focused on assemblages within the better exposed west-central and southern parts of the BGB (Anhaeusser, 1972, 1973, 1976; de Wit, 1982, 1983; de Wit et al., 1983; Lowe et al., 1985, 1999; de Wit et al., 1987b; Lamb and Paris, 1988; Lowe and Byerly, 1999). Stratigraphic relationships over the remaining sections of the belt are, for the most part, poorly resolved due to structural complications and a paucity of regional marker horizons which have only permitted broad lithostratigraphic correlations (Anhaeusser et al., 1983).

This paper presents results of mapping and associated geochemical studies conducted on greenstone assemblages in the northeastern sector of the BGB (Kohler, 1994, 2000). This work has led to the definition of a new lithostratigraphic unit, termed the Bien Venue Formation, within the upper Fig Tree Group.

REGIONAL GEOLOGIC SETTING

Stratigraphic Sequence and Ages

Rocks of the BGB have been subjected to multiple phases of deformation involving normal, reverse and strike-slip faulting, recumbent and upright folding, and granitoid activity (de Wit 1982, 1983; Jackson and Robertson, 1983; Anhaeusser, 1984; Lamb, 1984, 1987; Jackson et al., 1987; Heubeck and Lowe, 1994a, b; Kisters and Anhaeusser, 1995a, b; Lowe, 1999). The belt contains a complex arrangement of fault-bounded lithostratigraphic domains, which have been the subject of ongoing controversy for at least 20 years. The classic interpretations by Viljoen, M.J. and Viljoen (1969a, b) indicating a largely intact stratigraphic pile some 20 km thick were challenged by Williams and Furnell (1979), de Wit (1982, 1983), de Wit et al. (1983) and Lamb and Paris (1988) who suggested that the true thickness of the sequence was less than 5 km. More recent structural and isotopic studies, summarised in Lowe and Byerly (1999), have largely confirmed the classic stratigraphic interpretations, which form the basis of the present stratigraphic nomenclature (Fig. 2). All rocks within the BGB have been subjected

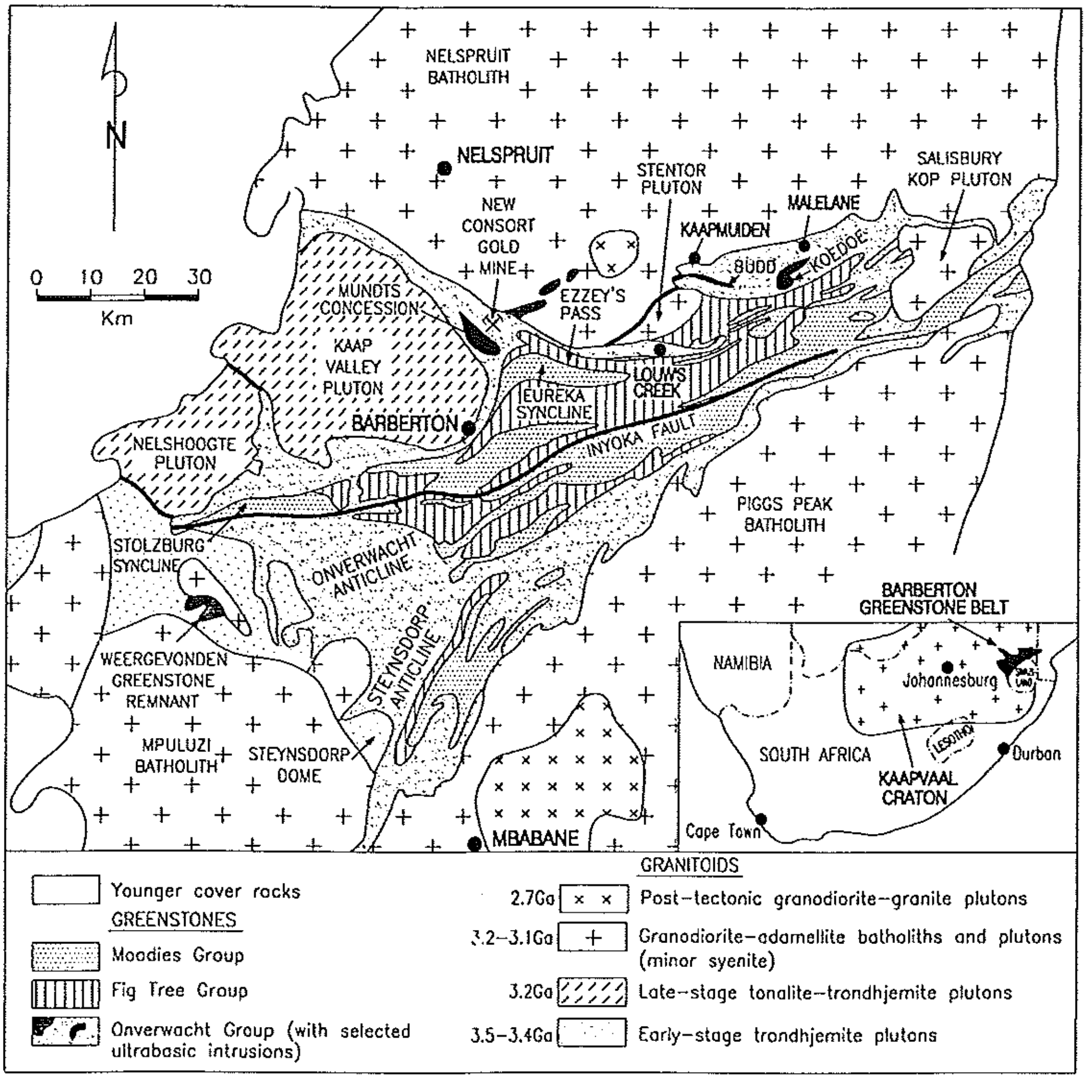

Figure 1: Generalised geological map of the Barberton greenstone belt and surrounding granitoid terrane (modified after Anhaeusser et al., 1983).

to metamorphism; the prefix "meta" is assumed, but has been omitted from lithologic descriptions given below.

In the southwest part of the belt, the Onverwacht Group, 8 to 12 km thick, has been subdivided into six formations (Viljoen, M.J. and Viljoen, 1969a,b; Viljoen, R.P and Viljoen, 1969a; Byerly, 1999; Lowe and Byerly, 1999). From the base up, these include:

(1) the Sandspruit Formation, composed of komatiite and komatiitic basalt;
(2) the Theespruit Formation, consisting mainly of basalt and komatiitic basalt, with intercalated units of silicic calc-alkaline pyroclastic and epiclastic rocks, now largely transformed to quartz-muscovite schists, and thin units of black and banded chert;
(3) the Komati Formation, characterised by interlayered komatiite and komatiitic basalt flows;
(4) the Hooggenoeg Formation, a sequence of tholeiitic basalt and komatiitic basalt, along with calc-alkaline silicic extrusive and high-level intrusive rocks at the top;
(5) the Kromberg Formation, which is dominated by basalt and basic volcaniclastic deposits, with minor komatiite; and
(6) the Mendon Formation, a sequence of interbedded komatiite, komatiitic basalt and cherty rocks.

<table>
<tr><th colspan="2"></th><th colspan="2">Southern and Central Domains</th><th>Northern Domain</th><th>Northeastern Domain (this study)</th></tr>
<tr><td rowspan="13">Swaziland Supergroup</td><td rowspan="3">Moodies Group</td><td rowspan="3" colspan="2">Undivided Moodies Group</td><td>Baviaanskop Fm</td><td rowspan="3">Undivided Moodies Group</td></tr>
<tr><td>Joe's Luck Fm</td></tr>
<tr><td>Clutha Fm</td></tr>
<tr><td rowspan="4">Fig Tree Group</td><td rowspan="4">Mapepe Fm</td><td rowspan="4">Auber Villiers Fm</td><td>Schoongezicht Fm</td><td>? ? ?</td></tr>
<tr><td rowspan="2">Belvue Road Fm</td><td>Bien Venue Fm</td></tr>
<tr><td>Belvue Road Fm</td></tr>
<tr><td>Sheba Fm</td><td>Sheba Fm</td></tr>
<tr><td rowspan="6">Onverwacht Group</td><td colspan="2">Mendon Fm</td><td>Weltevreden Fm</td><td>Weltevreden Fm</td></tr>
<tr><td colspan="2">Kromberg Fm</td><td rowspan="5">? ? ?</td><td rowspan="5">? ? ?</td></tr>
<tr><td colspan="2">Hooggenoeg Fm</td></tr>
<tr><td colspan="2">Komati Fm</td></tr>
<tr><td colspan="2">Theespruit Fm</td></tr>
<tr><td colspan="2">Sandspruit Fm</td></tr>
</table>

Figure 2: *Stratigraphic classification of rocks of the Barberton greenstone belt south (Southern and Central Domains) and north (Northern Domain) of the Inyoka Fault (modified after Lowe and Byerly, 1999). Also shown is the stratigraphic classification of rocks in the northeastern sector of the belt (Northeastern Domain). The position of the Bien Venue Formation, discussed in this paper, is highlighted in bold type. Note: Diagram not to scale.*

Assemblages of the Onverwacht Group in the northern part of the belt have been variously assigned to the Theespruit or Komati Formations (Viljoen and Viljoen, 1970; Anhaeusser, 1972, 1976; Anhaeusser et al., 1983), or to a new unit, the Weltevreden Formation, composed largely of komatiite and komatiitic basalt intruded by layered ultrabasic bodies, which appears to correlate with the Mendon Formation (Lowe and Byerly, 1999; Lowe et al., 1999).

The Onverwacht Group formed over a period of 270 Ma between ca 3550 – 3280 Ma. Silicic volcaniclastic rocks of the Theespruit Formation in the Onverwacht anticline have an age of 3453 ± 6 Ma (Armstrong et al., 1990). However, dating of quartz-muscovite schists, correlated with the Theespruit Formation in the Steynsdorp area, has indicated significantly older ages of 3544 ± 3 Ma to 3548 ± 1.3 Ma (Kröner et al., 1996). Assemblages within the Hooggenoeg Formation have been dated at 3452 ± 3 Ma to 3438 ± 12 Ma (Kröner and Todt, 1988; Armstrong et al., 1990; Kröner et al., 1991; Byerly et al., 1996). The ages of the Mendon and Weltevreden Formations are constrained at 3298 ± 3 Ma and 3286 ± 29 Ma, respectively (Lahaye et al., 1995; Byerly et al., 1996).

The Fig Tree Group conformably overlies the Onverwacht rocks and attains a thickness of ~3 km. The Group contains two distinct facies, a southern shallow-water facies, south of the Inyoka fault, and a deeper-water northern facies. The southern facies includes two formation-level units:

(1) the Mapepe Formation, composed of ferruginous shale, greywacke, banded iron-formation (BIF), jaspillite, sandstone and conglomerate, along with precipitative barite horizons and fine-grained distal dacitic tuffaceous rocks (Nocita and Lowe, 1990; Lowe and Nocita, 1999); and
(2) the Auber Villiers Formation, which structurally overlies the Mapepe Formation, and consists of plagioclase-phyric dacitic epiclastic material, locally with interbedded turbidites and chert- and shale-clast conglomeratic units (Lowe and Byerly, 1999).

In the northern part of the belt Condie et al. (1970) and Lowe and Byerly (1999) subdivided the Fig Tree Group, from base to top, into three formations, viz:

(1) the Sheba Formation, a sequence of interbedded turbiditic greywacke, siltstone and BIF;
(2) the Belvue Road Formation, which includes shale and siltstone, with minor greywacke and BIF, and sporadic lenses of dacitic epiclastic rocks; and
(3) the Schoongezicht Formation, which is characterised by a proximal sequence of plagioclase-phyric dacitic volcaniclastic rocks, including tuffs, turbidites and coarse-textured conglomeratic units.

Rocks of the Mapepe and Auber Villiers Formations have yielded ages of 3258 ± 3 Ma to 3227 ± 4 Ma, and 3256 ± 4 Ma and 3253 ± 3 Ma, respectively (Kröner et al., 1991; Byerly et al., 1996), suggesting that these two units are, at least in part, age equivalents. The Schoongezicht Formation has been dated at 3226 ± 1 Ma to 3222 +10/-4 Ma (Kröner et al., 1991; Kamo and Davis, 1994).

The Moodies Group, up to 3.7 km thick, consists of arkosic, lithic and quartzose sandstone, and polymictic conglomerate, with subordinate siltstone, shale, jaspillite and volcanic rocks (Anhaeusser, 1976; Heubeck and Lowe, 1999). Deposition and deformation of Moodies strata has been bracketed between 3224 ± 6 Ma and 3109 +10/-8 Ma (Heubeck et al., 1993; Heubeck and Lowe, 1994a).

Granitoid Rocks

The BGB is surrounded by several generations of tonalite-trondhjemite-granodiorite (TTG) plutons, multi-component granodiorite-adamellite batholithic complexes, and late-stage, largely post-tectonic, granodiorite and granite plutons (Anhaeusser and Robb, 1981). Early TTG suites along the southwest margin of the belt range in age from 3460 ± 6 Ma to 3437 +5/-4 Ma, with the exception of the Steynsdorp dome, which has been dated at 3510 ± 4 Ma to 3502+/-2 Ma (Armstrong et al., 1990; Kröner et al., 1991; Kamo and Davis, 1994; Kröner et al., 1996). Late TTG plutons west of the belt include the Kaap Valley and Nelshoogte plutons that have been dated at 3229 ± 5 Ma to 3212 ± 2 Ma (Tegtmeyer and Kröner, 1987; Armstrong et al., 1990; Kamo and Davis, 1994; Layer et al., 1998). The Mpuluzi and Nelspruit granodiorite-adamellite batholithic complexes south and north of the BGB have been radiometrically constrained at 3107 +4/-2 Ma and 3106 ± 3 Ma, respectively (Kamo and Davis, 1994). The Salisbury Kop pluton, which intrudes assemblages in the extreme northeastern part of the belt, has been dated at 3109 +10/-8 Ma to 3079 ± 6 Ma (Heubeck et al., 1993; Kamo and Davis, 1994). Late-stage plutons in the region postdate the emplacement of the Mpuluzi and Nelspruit batholiths by 360 to 400 Ma (Layer et al., 1989; Maphalala and Kröner, 1993).

Structure and Alteration

The greenstone pile has been subjected to a protracted period of folding and faulting, with up to five separate phases of deformation recognised (de Wit, 1982; de Wit et al., 1983; Lamb, 1984; de Ronde and de Wit, 1994; Heubeck and Lowe, 1994b; Lowe et al., 1999). Primary layering is near-vertical throughout much of the belt, and overturning of stratigraphic units is common. The structural architecture of the belt is dominated by a series of northeast-striking tight-to-isoclinal, upright and north-verging folds that are bounded by subvertical to south-dipping faults showing components of normal, reverse and strike-slip motion. Deformation of a more localised nature accompanied the emplacement of magmatic and solid-state diapirs along the margins of belt (Anhaeusser, 1984; Kisters and Anhaeusser, 1995a,b).

Alteration of the greenstone lithologies involved the superposition of successive sea-floor alteration, regional burial and dynamic contact metamorphic events (Cloete, 1999). In general, metamorphic grade of the rocks ranges from the amphibolite facies in marginal areas flanking major granitic intrusions to subgreenschist in the central parts of the belt.

GEOLOGY OF THE NORTHEASTERN SECTOR OF THE BGB

Greenstones

Aspects of the stratigraphy and structural geology of the greenstones in the northern and northeastern sectors of the BGB have previously been described by Viljoen and Viljoen (1970), Anhaeusser (1972, 1976, 1986b) and, most recently, by Kohler (1994, 2000), so that only a brief summary is given here (Fig. 3).

Onverwacht Group

The Onverwacht Group is made up largely of fine-grained basic and ultrabasic schists, including amphibole-, chlorite- and talc-bearing varieties, with subordinate massive serpentinite, foliated amphibolite and silicic schist. These rocks crop out along the granitoid-greenstone interface between Louw's Creek and the Jamestown Schist Belt, west of the New Consort gold mine, and also in the area south and southeast of Kaapmuiden (Fig. 1).

Primary textures are seldom preserved, however, geochemical and petrographic data suggest that the rocks were derived from a precursor suite that ranged in composition from komatiite and komatiitic basalt through to basalt and dacite-rhyodacite (Viljoen and Viljoen, 1970; Kohler, 1994). Also present within the sequence are a number of large, generally differentiated, ultrabasic sills composed of altered dunite, pyroxenite, gabbro and anorthosite (Anhaeusser, 1985, 1986a). South and east of Kaapmuiden, these bodies include the Budd and Koedoe layered intrusions (Viljoen and Viljoen, 1970). The Mundt's Concession intrusion, which is exposed in the eastern part of the Jamestown Schist Belt (Anhaeusser, 1972), has been dated by the Pb-Pb whole rock technique at 3 244 ± 140 Ma (Dupré and Arndt, 1990).

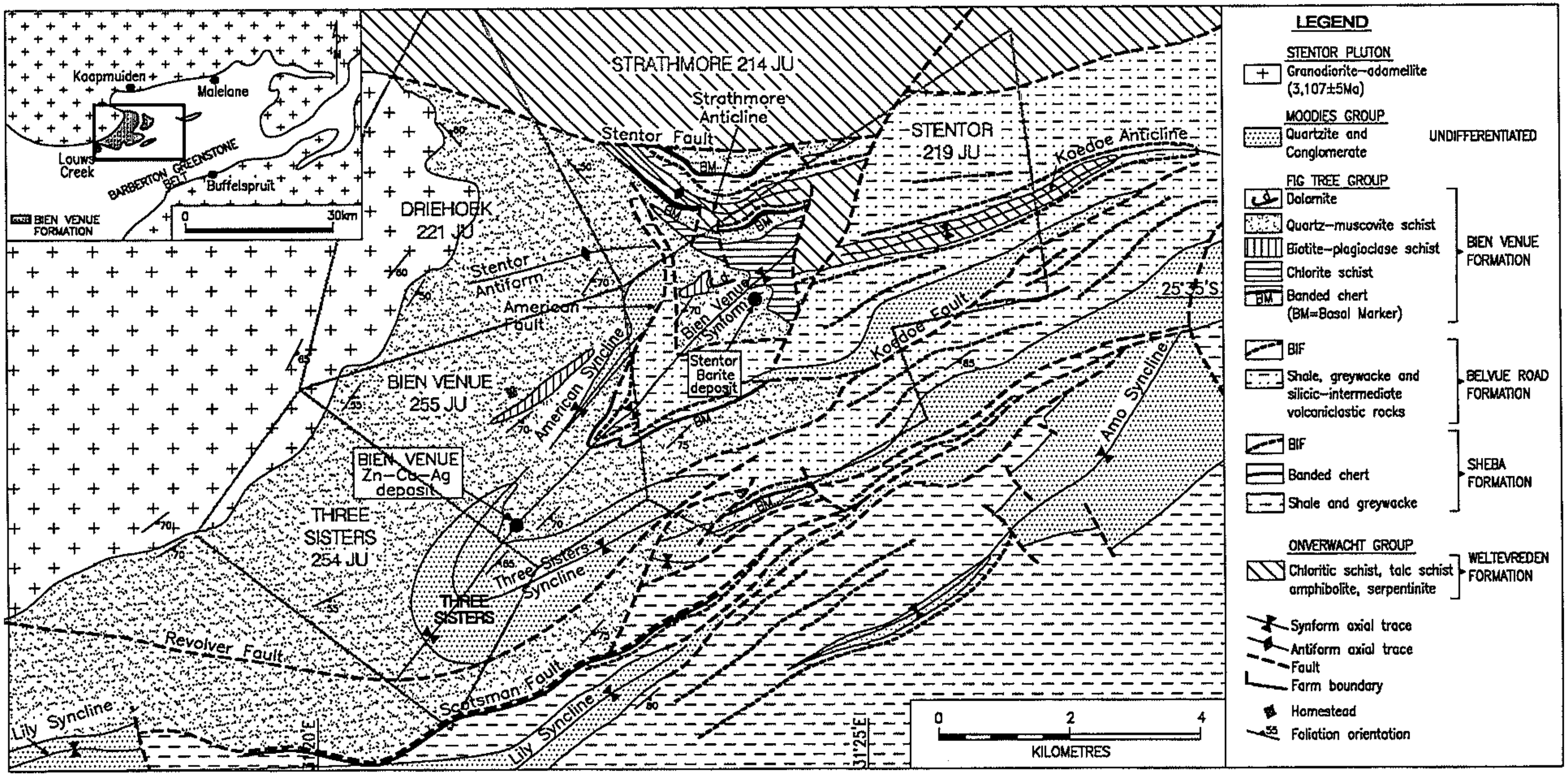

Figure 3: Simplified geological map of the northeastern part of the Barberton greenstone belt in the vicinity of Three Sisters.

Rocks of the Onverwacht Group southeast of Kaapmuiden have previously been correlated with the Komati Formation (Viljoen and Viljoen, 1970), whereas those west of Louw's Creek have been assigned to the Theespruit Formation (Anhaeusser, 1972). Based on the recent stratigraphic re-correlation of units north of the Inyoka fault (Lowe and Byerly, 1999), coupled with the abovementioned, albeit imprecise, age for the Mundt's Concession intrusion, it now seems likely that these rocks belong to the Weltevreden Formation, although further age dating will be required to confirm this preliminary interpretation.

Exposures of Onverwacht rocks, largely comprising metamorphosed basalt and minor gabbro, also occur in the core zones of anticlinal structures within the greenstones, and as xenolithic remnants, up to 3 km long, within gneissic rocks of the Nelspruit batholith (Kohler, 1994). The xenoliths have been contact metamorphosed to amphibolite, and locally contain massive and foliated serpentinite derived from komatiite. The precise stratigraphic position of these units is not clear, but they are also tentatively assigned to the Weltevreden Formation.

Fig Tree Group

The Fig Tree Group comprises successions of turbiditic shale-slate and greywacke, a thick accumulation of heavily altered silicic-intermediate volcanic-volcaniclastic rocks, and minor intercalated BIF, chert and basic-ultrabasic units. Correlation of the shale and greywacke assemblages with either the Sheba or Belvue Road Formations is hampered by structural complexities and, locally, inadequate exposure, partly due to afforestation. Greywacke sequences are well developed east of Louw's Creek, and the rocks in this region have been tentatively correlated with the Sheba Formation. Fig Tree assemblages northeast of Three Sisters, on the other hand, contain a greater proportion of shale and, in places, also lenticular units of altered silicic-intermediate volcaniclastic rock, composed of quartz-feldspar-muscovite ± pyrophyllite, or tuffaceous shale and siltstone, and have accordingly been assigned to the Belvue Road Formation.

Field relationships outlined in subsequent sections of this paper indicate that argillaceous assemblages of the Belvue Road Formation in the northeastern part of the BGB are overlain by a sequence of silicic schists. These rocks, previously correlated by Viljoen and Viljoen (1970) with the Theespruit Formation, are, in turn, overlain by arenaceous and rudaceous units of the Moodies Group. The schists appear to occupy the same *apparent* stratigraphic position in the Swaziland Supergroup as the Schoongezicht Formation, and have accordingly been correlated with the Fig Tree Group. However, despite similarities in apparent stratigraphic position, significant age and lithologic differences preclude direct correlation with the Schoongezicht Formation. Accordingly, the schists have been assigned to a new stratigraphic unit, termed the Bien Venue Formation.

Moodies Group

Alluvial to shallow-marine strata of the Moodies Group unconformably, paraconformably and structurally overlie rocks of both the Fig Tree and Onverwacht Groups. The succession is dominated by interbedded conglomerate and quartzite, grading upwards into quartzite, pebbly quartzite and, in places, siltstone, shale and BIF. Owing to a lack of suitable marker horizons, correlation of Moodies rocks from syncline to syncline, or with units outside the present study area is generally not feasible.

Granitoid Rocks

The granitoid terrane north of the BGB comprises a heterogeneous suite of strongly foliated, trondhjemitic-to-granitic (sensu stricto) gneisses and migmatites forming part of the Nelspruit Migmatite and Gneiss Terrane, the latter interpreted as the basal zone of the Nelspruit batholith (Robb et al., 1983). These gneisses are accompanied by medium- to coarse-grained, equigranular granodiorite-to-adamellite of the Stentor pluton, which also forms part of the Nelspruit batholith (Kohler, 1994). The Stentor pluton has been dated at 3107 ± 5 Ma (Kamo and Davis, 1994), and intruded the rocks of the Bien Venue Formation as a hot diapir.

Structure

The deformational history of the northeastern sector of the BGB was dominated by a north-northwestward-directed compressional tectonic regime. This deformation gave rise to a series of major, east-northeast-trending, tight-to-isoclinal, upright and northwest-verging folds, and imposed a penetrative, subvertical- to steeply dipping axial planar cleavage, S_1, on the rocks. The folds are bounded by strike-extensive, generally near-vertical or steep southeast-dipping faults. These faults generally lie parallel the fold axial traces, but locally obliquely crosscut the fold limbs and axial traces.

In the vicinity of the Three Sisters peaks, post-Moodies Group compressional deformation gave rise to the Three Sisters and American synclines. In both of these synclines, Moodies Group conglomerates and quartzites stratigraphically overlie silicic schists of the Bien Venue Formation. The American syncline is a tight, steeply inclined fold that plunges ~70° east-southeast. The fold axial surface dips 70° south-southeast. Sedimentary indicators of younging confirm that the structure is upward-facing. At its northern end, the syncline is bounded on the eastern side by the American fault, which progressively cuts across the strike of the rocks, juxtaposing shale and BIF assemblages of the Belvue Road Formation against the Moodies rocks. East of the American fault, the Barite fault juxtaposes the Belvue Road lithologies against a second package of silicic schists correlated with the Bien Venue Formation.

The Three Sisters syncline is a complex, mainly east-northeast-trending tight fold that has been modified by later deformation. The eastern section of the fold plunges 60° south-southeast, with an axial surface inclined ~70° southeast. The western part of the structure trends at an angle to the main body of the syncline due to later refolding. To the south, the Three Sisters syncline is bounded by basic schists of the Weltevreden Formation along the Revolver fault, a late-stage structure that postdates the Stentor pluton (Kohler, 1994).

Deformation of a more localised nature accompanied the diapiric emplacement of the Stentor pluton. This deformation led to the formation of two major fold structures, the Stentor antiform and the Bien Venue synform, and imposed an intensely developed schistosity, S_2, on rocks west of the pluton. The Stentor antiform is open in form and upright, and plunges ~50° east-northeast. All rocks within the antiform are pervasively, but heterogeneously, deformed and altered, showing few preserved primary textures. S_2 has a pronounced arcuate trend parallel to the Stentor pluton contact, with moderate-to-steep (50°-75°) dips to the east, southeast or northeast. S_2 also lies subparallel to primary layering, where discernible, within the silicic sequences. Strain intensity can be directly related to proximity to the Stentor pluton; S_2 fabrics are best-developed in schists along the granitoid contact and progressively diminish in intensity eastwards.

The Bien Venue synform is a tight, steeply inclined fold that plunges ~60° south-southeast. Unambiguous indicators of younging direction are rare within the structure, but the distribution of units north of the Three Sisters peaks indicates that it is downward-facing. The synform was responsible for the refolding of the western section of the Three Sisters syncline. The refolding event is also interpreted to have led to the reorientation of the American syncline, which probably originally lay west of the main body of the Three Sisters syncline, and may well have represented the westerly continuation of the latter structure. A number of prominent Z-, S- and W-type parasitic folds have developed along the limbs and in the hinge zone of the Bien Venue synform. S_2 dips uniformly southeast at 45°-75°, parallel to the axial surface, and crosscuts primary layering.

BIEN VENUE FORMATION

Geological Setting

The Bien Venue Formation is composed almost entirely of quartz-muscovite schists derived from silicic volcanic-volcaniclastic precursors, and represents the single most aerially extensive accumulation of such rocks in the BGB, covering 50 km^2. The principal exposures occur in the Stentor antiform and the Bien Venue synform on the farms Bien Venue 255 JU, Driehoek 221 JU and Stentor 219 JU. Sporadic outcrops of silicic volcaniclastic rock, believed to form part of the Bien Venue Formation, also occur southwest of the town of Malelane.

The quartz-muscovite schists overlie a prominent grey-and-white banded chert, informally named the Basal Marker, which, in most areas, conformably rests on rocks of the Belvue Road Formation. Lenses of biotite-plagioclase schist, chlorite schist, talc schist, phyllite-slate and cherty dolomite form a minor component of the stratigraphy. Although these rocks constitute the only easily recognisable units within the generally highly sheared succession, their discontinuous nature precludes their use as marker beds on a regional-scale. On Bien Venue 255JU and Stentor 219JU, the quartz-muscovite schists host subeconomic barite and base-metal massive sulphide mineralization (Fig. 3).

The lack of suitable marker horizons does not allow an estimate of the amount of structural repetition within the formation. However, it is believed that tectonic thickening may be considerable within the core of the Bien Venue synform, and adjacent to the Stentor pluton. No definitive section of the entire formation can be defined, and the thickness of the original volcanic-volcaniclastic pile cannot readily be determined. Total structural thickness of the formation along the southeast limb of the Bien Venue synform is approximately 700 m, but may be as thick as 3000 m on the southern limb of the Stentor antiform.

Quartz-muscovite Schists

The quartz-muscovite schists of the Bien Venue Formation display lithologic similarities with silicic schists elsewhere in the BGB. The schists are fine- to medium-grained, and give rise to an arcuate belt of hills overlooking the Stentor pluton to the west. Fresh surfaces are buff or greyish-green, but weathered surfaces are tan or pale rusty brown due to iron staining. Silicification of the schists is intense in the core of the Bien Venue synform and along the contact of the Stentor pluton.

Despite intense tectono-hydrothermal alteration, relic textures attesting to a volcanic or volcaniclastic protolith are frequently recognisable in the field. By far the most common primary textures are stubby, pre-kinematic insets of colourless or light-blue quartz. These insets represent relic ß-quartz phenocrysts or pyrogenic grains, and impart a weak- to well-developed porphyroclastic texture to the rocks. The porphyroclasts generally range between 1-5 mm in size, and locally comprise an estimated 30 % or more of the total volume of some specimens. Schistose units containing dense-packed aggregates of angular quartz insets, locally interbedded with narrow lenses of ferruginous shale, were probably derived from crystal-rich volcaniclastic sandstones.

Schists showing relic clasts of recrystallized, granular-textured chert or, more rarely, fine-textured silicic metavolcanic (quartz-muscovite) rock, are best developed on a ridge south of the homestead on Bien Venue 255JU, where they form discontinuous units traceable laterally for a few hundred metres (Fig. 4a and b). The metavolcanic clasts are compositionally identical to the surrounding matrix. The clasts are generally poorly sorted, range from subangular to rounded, but are typically highly deformed; long axes of ellipsoidal clasts tectonically flattened in the plane of the foliation define a prominent down-dip stretching lineation. Clast sizes range from 1-15 cm.

In addition to quartz and muscovite, schists along the Stentor pluton contact frequently contain andalusite, biotite and pyrophyllite, and are coarser-textured than schists further away from the granitoid contact, which contain variable proportions of chlorite, chloritoid, andalusite, biotite and pyrophyllite. Minor phases include calcite, plagioclase, microcline, zircon, apatite, tourmaline, epidote and magnetite.

Quartz commonly accounts for 50-65 % of the total volume of the schists. The bulk of the quartz occurs as xenoblastic microcrystalline grains. The remainder forms the previously described insets, which display angular-to-rounded, commonly deeply embayed shapes. Hexagonal bipyramidal crystals are comparatively rare. Most insets show strain phenomena, including radiating extinction, quartz-infilled pressure shadows, boudinage structures, deformation lamellae and partial recrystallization. Intensely strained and recrystallized insets along the granitoid contact occur as lensoid aggregates or ribbons of mosaic-textured quartz, parallel to S_2.

Muscovite occurs as finely disseminated, aligned laths or sheaf-like aggregates defining S_2, and generally accounts for 25-40% of the rock volume. Relic crystals of plagioclase (albite - oligoclase) and, less commonly, microcline, invariably showing deformation and extensive replacement by fine-grained muscovite, occur in least-altered samples.

Andalusite may constitute up to 15% of the rocks, and forms xenoblastic porphyroblasts and poikiloblasts up to 4 mm in size. Andalusite poikiloblasts contain straight or sigmoidal inclusion trails defined primarily by quartz and opaque phases (Fig. 5a). Microstructural relationships indicate that andalusite growth occurred both during and after formation of S_2. Pyrophyllite occurs as a fine-grained postkinematic retrograde replacement product of andalusite along grain boundaries, cleavage planes and microfractures (Fig. 5b). Chloritoid forms small (0.1 - 2 mm long), subidioblastic-to-idioblastic porphyroblasts that account for over 15% of some specimens. Isolated crystals showing pronounced multiple twinning are most common, but radial and fan-shaped aggregates composed of several crystals also occur

(a)

(b)

Figure 4: *Preserved conglomeratic textures in quartz-muscovite schist. (a) Strongly flattened and recrystallized chert clasts. Plane of view is parallel to S_2. (b) Relic clasts of (altered) volcanic material. Plane of view is approximately orthogonal to S_2. Lens caps = 5 cm wide.*

(Fig. 5c). Chloritoid growth was dominantly postkinematic with respect to S_2, but some growth was synkinematic. Biotite forms isolated ragged flakes intergrown and aligned with muscovite and chlorite, but is occasionally found in monomineralllic clusters. Chlorite occurs as discrete, synkinematic xenoblastic flakes and wispy aggregates, intergrown with, and replacing, muscovite. Some chlorite is also found as a retrograde product rimming chloritoid and biotite.

Poorly exposed, but least-deformed rocks south of Malelane are characterised by abundant euhedral-to-subhedral plagioclase, microcline and perthite crystals, typically ~0.1 - 1 mm across, showing variable alteration to muscovite. Some specimens contain large quartz insets, similar in size and shape to least deformed insets north of Three Sisters. Surrounding the crystals is a fine-grained, isogranular - to - lepidoblastic groundmass composed of quartz,

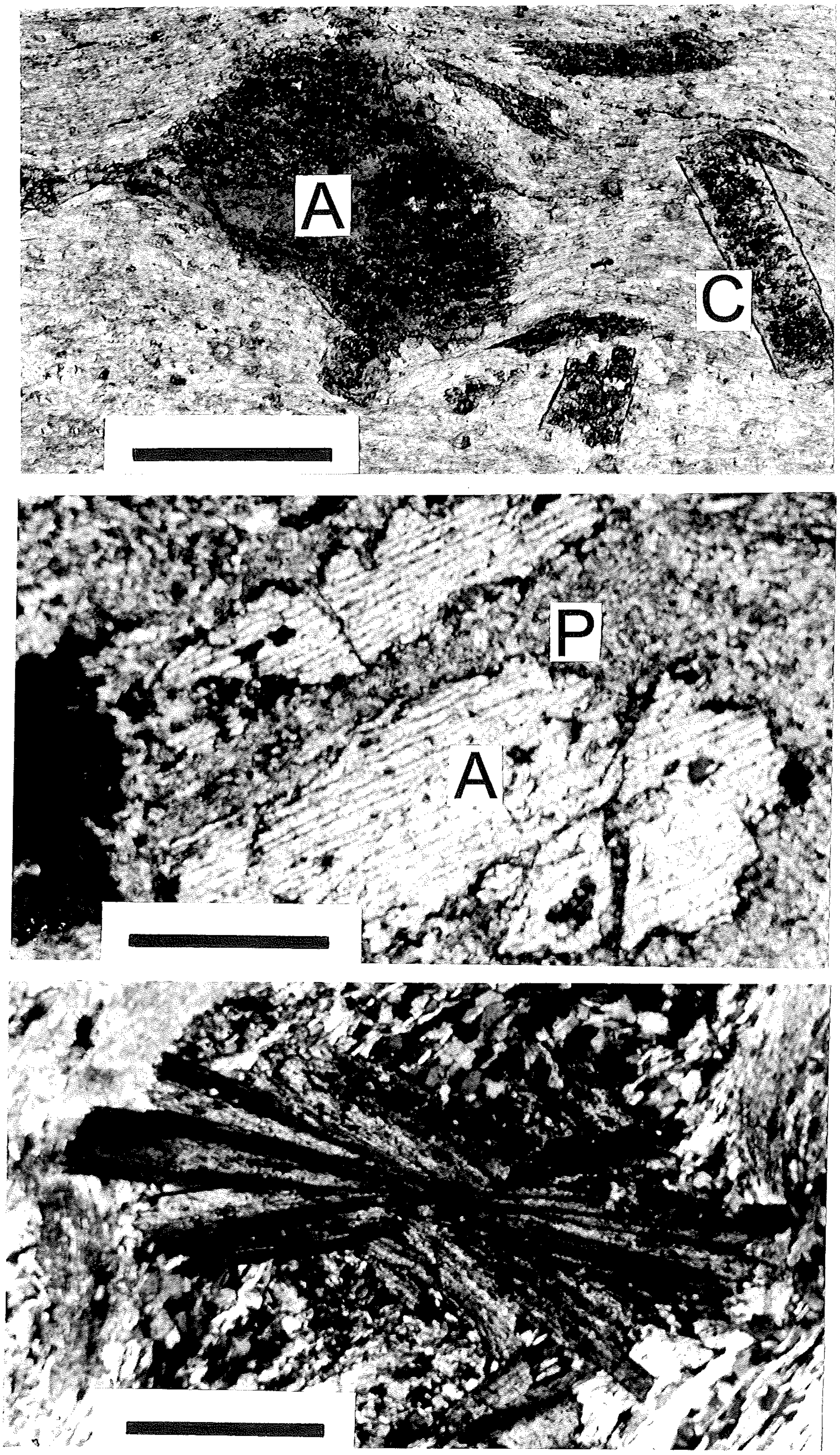

(a)

(b)

(c)

Figure 5: Petrographic features of quartz-muscovite ± andalusite ± chloritoid ± pyrophyllite schists. (a) Andalusite poikiloblast (A) with sigmoidal quartz inclusion trails. A late-stage chloritoid crystal (C) has grown across the inclusion trails. (b) Andalusite porphyroblast (A) showing peripheral alteration to pyrophyllite (P). (c) "Hour-glass" aggregate of chloritoid crystals oriented at high angle to S_2, with evidence of post-chloritoid flattening. Bar scales = 30 mm.

feldspar, calcite, muscovite and chlorite, with accessory apatite, epidote - clinozoisite, zircon and iron oxides. Relic ash- and lapilli-sized fragments of silicic volcanic material range from angular to subrounded, and are usually characterised by abundant, unoriented feldspar microphenocrysts. With increasing deformation and alteration, the fragments as well as the enveloping groundmass show progressive replacement by muscovite.

Biotite-plagioclase Schists

Dark-grey to grey-green weathering schists consisting mainly of biotite, but also characteristically containing abundant plagioclase (mainly albite-oligoclase) insets to ~7 mm long, outcrop at several localities. The principal exposures of these rocks lie immediately east of the homestead on Bien Venue 255 JU, forming a conspicuous, 200 m wide and 1.8 km long, northeast-striking lens-shaped unit, intercalated within, and containing minor intercalations of, quartz-muscovite schist. In places, the rocks contain distinctive light-grey lenticular structures with long axis dimensions to 40 cm (Fig. 6). These structures are invariably aligned parallel to S_2, suggesting that their present-day morphology is due to tectonic flattening rather than a primary feature. They closely resemble the clasts of plagioclase-phyric dacitic material found in conglomerates within the Schoongezicht Formation (Condie et al., 1970; Lowe and Byerly, 1999). In some exposures, the schists also contain isolated, but usually strongly tectonically flattened, clasts of recrystallized chert, or more rarely, medium-textured quartz-feldspar porphyry.

Figure 6: *Flattened relic dacitic metavolcanic clasts in biotite-plagioclase schist. Plane of view is approximately orthogonal to S_2. Lens cap = 5 cm.*

The plagioclase insets occur as discrete, euhedral-to-rounded, occasionally embayed, but commonly fractured and sericite-dusted pre-kinematic crystals that usually account for 15-40 % of the volume of rocks. Biotite constitutes the main groundmass mineral defining S_2, which wraps around the feldspars. Chlorite, calcite, quartz and epidote occur as fine-grained xenoblastic grains intergrown with biotite. Accessory minerals include titanite, apatite and zircon.

Chlorite- and Talc Schists

The principal exposures of basic schist occur along the northern boundary of Stentor 219 JU. Here the rocks form a 150-250 m wide and 1.5 km long, northwest-striking band capped by a 1-2 m-thick recrystallized chert. The basic unit attains its fullest development in the vicinity of the Stentor barite deposit where it has been affected by W-type parasitic folding associated with the Bien Venue synform. The schists consist largely of chlorite, with lesser amounts of quartz, tremolite - actinolite and carbonate. Euhedral-to-subhedral, but generally fractured, relic plagioclase crystals are common. Minor constituents include titanite, biotite, epidote and magnetite.

Ankle-high outcrops of highly weathered, greyish-green ultrabasic schist composed of talc, chlorite and carbonate occur in a thin (5-20 m wide), poorly exposed band underlying the main chlorite schist unit.

Cherts and Dolomites

Chert units occur as a minor component throughout the Bien Venue Formation, but are best developed along the lower contact, forming the Basal Marker. This unit ranges in thickness from 1 - 350 m, and consists of banded black, brown and white chert, grading into zones of massive- to finely laminated grey chert. The bands are 0.1-3 cm wide, but can be as thick as 15 cm. The rocks consist of recrystallized, polygonal-textured micro-quartz, with minor muscovite, feldspar, chlorite, carbonate, epidote and iron oxide. The darker coloration of the grey bands reflects the presence of fine disseminations of amorphous carbon and graphite. Chert breccias occur as thin (mostly less than 30 cm wide) conformable units containing slab-like clasts of white chert enclosed by a dark-grey cherty matrix.

In places, the Basal Marker contains intercalations of laminated shale, turbiditic sandstone and silicic volcaniclastic rocks. Thickness of these intercalations is usually in the centimetre to decimetre range, but can be up to several metres, and in rare instances, tens of metres. Replacement of the contained tuffaceous and argillaceous units by irregular crosscutting veinlets and stockworks of grey chert is common. Highly siliceous bands locally preserve small-scale sedimentary structures, such as low-angle cross-bedding, and ghost outlines of original detrital particles.

Less common than the cherts are cherty carbonate units. Outcrops of these rocks are generally poor and very discontinuous. The best exposures occur 700m west of the Stentor barite deposit. Here, the carbonate rocks form a 5m wide and 250m long marker unit outlining the hinge of a small isoclinal fold. Outcrops show crude, but generally subparallel bands of recrystallized dark-brown dolomite and grey chert 5-50 cm thick. Contacts between individual dolomite and chert layers are irregular, with thin veinlets of the latter penetrating the former and visa versa. Elsewhere, the rocks have undergone severe deformation and recrystallization, and consequently do not display the layering seen west of the Stentor deposit.

Phyllites and Slates

Laterally impersistent lenses of brown- and grey-weathering phyllite and slate are interlayered with the quartz-muscovite and, less commonly, biotite-plagioclase schists. Thickness of these units is in the decimetre-to-metre range, but is locally several tens of metres. The slates form inconspicuous outcrops, generally over strike lengths of less than 50 m. The rocks consist of angular silt-sized quartz and rare feldspar grains set in a fine-grained, often carbonaceous, muscovite- and chlorite-rich matrix. Interbeds of fine- to medium-grained volcaniclastic sandstone, possibly of turbiditic origin, and quartz-muscovite schist are found in some of the thicker units. Rare low-angle cross-bedding is present in some of the sandstone beds. In some outcrops, the argillites contain abundant scattered quartz insets, identical to those in the quartz-muscovite schists, or less commonly, strongly flattened pebble-sized clasts of recrystallized chert.

Barite Deposit

Quartz-muscovite schists in the Stentor area host subeconomic barite mineralization (Viljoen, R.P. and Viljoen, 1969b; Reimer, 1980). The barite occurs as thin (1 - 15 cm wide), pale-green or grey-coloured interlayers and lenses within a steep- to subvertically dipping sequence of chert. Specimens contain fine-grained, granular masses of turbid barite, along with minor amounts of quartz, carbonate, pyrite, chalcopyrite and iron-oxides. According to Reimer (1980), the mineralized zone extends over a stratigraphic height of 70 m and is traceable along strike for about 700 m. Reimer (1980) also reported the presence of faint cross-laminations and rounded chert fragments in some of the barite layers, suggesting that the mineralization formed syngenetically in a shallow-marine environment.

Correlation of the Stentor barite deposit, which was originally thought to occur in rocks of the lower Onverwacht Group (Viljoen and Viljoen, 1969b; Reimer, 1980), with the Bien Venue Formation, makes this occurrence somewhat unique in the BGB. In contrast to barite deposits in the southern facies of the Fig Tree Group, notably in the Mapepe Formation, which occur in terrigenous clastic sequences (Heinrichs and Reimer, 1977; Lowe and Nocita, 1999), the Stentor mineralization is hosted by sheared volcanic-volcaniclastic rocks, a setting more commonly associated with the Theespruit Formation.

Massive Sulphide Deposit

The Bien Venue volcanogenic massive sulphide (Zn-Cu-Ag) deposit is situated in the hinge zone of the Bien Venue synform, close to the contact with Moodies strata coring the Three Sisters syncline. The results of the exploration programme are confidential, so that the writers do not know the size or grade of the deposit. The host rocks, as well as the contained sulphide zones, have been subjected to folding. On surface, the mineralization is manifest as a poorly exposed, V-shaped zone of gossan and gossanous quartz-muscovite schist, traceable over a strike length of approximately 300 m. The bulk of the sulphides occur in near-vertical, massive and semi-massive lenses within a 50-70 m wide mineralised zone (Harwood and Murphy, 1988; Murphy, 1990). The lenses consist of extensively recrystallized fine-grained pyrite and sphalerite, together with variable, but lesser, amounts of galena, tennantite, chalcopyrite and covellite. Sphalerite and galena are preferentially concentrated towards the stratigraphic hangingwall of the deposit. Native silver and copper-silver sulphides, including jalpaite and mackinstryite, occur interstitially. The sulphides often occur in stringers aligned parallel the host rock axial-planar S_2 schistosity, suggesting that the recrystallization accompanied metamorphism and deformation. Fine disseminations of pyrite and chalcopyrite are present in the immediate footwall, while thin (less than 1 m wide), laterally impersistent barite, chert and dolomite layers characterise the uppermost portions of the mineralised zone. Despite extensive recrystallization, preserved textural evidence suggests that the sulphide mineralization formed from Kuroko-like sea-floor exhalative activity (Murphy, 1990).

METAMORPHIC ALTERATION

Rocks of the Bien Venue Formation north and west of Three Sisters have been affected by syndeformational contact metamorphic alteration linked to the intrusion of the Stentor pluton. The alteration led to pronounced mineralogical and chemical transformations to the precursor rocks of the quartz-muscovite schists, specifically a change from a primary mineralogy of quartz + plagioclase + K-feldspar + ferromagnesian silicates to a secondary assemblage of quartz + muscovite ± andalusite ± chlorite ± chloritoid ± biotite ± pyrophyllite. Sillimanite and staurolite have been reported from quartz-muscovite schists close to intrusive granitoids elsewhere along the northern flank of the BGB (Anhaeusser, 1972, 1986b), but have not been recorded in specimens from the Bien Venue Formation.

The breakdown of plagioclase and K-feldspar to muscovite can be attributed to hydrolysis reactions of the following kind:

$$\underset{\text{K-feldspar}}{3KAlSi_3O_8} + 2H^+ = \underset{\text{muscovite}}{KAl_3Si_3O_{10}(OH)_2} + \underset{\alpha\text{-quartz}}{6SiO_2} + 2K^+$$

$$\underset{\text{plagioclase (albite fraction)}}{3NaAlSi_3O_8} + 2H^+ + K^+ = \underset{\text{muscovite}}{KAl_3Si_3O_{10}(OH)_2} + \underset{\alpha\text{-quartz}}{6SiO_2} + 3Na^+$$

$$\underset{\text{plagioclase (anorthite fraction)}}{3CaAl_2Si_2O_8} + 4H^+ + 2K^+ = \underset{\text{muscovite}}{2KAl_3Si_3O_{10}(OH)_2} + 3Ca^{2+}$$

Andalusite appears to have formed from the hydrolysis of muscovite:

$$\underset{\text{muscovite}}{2KAl_3Si_3O_{10}(OH)_2} + 2H^+ = \underset{\text{andalusite}}{3Al_2SiO_5} + \underset{\alpha\text{-quartz}}{3SiO_2} + 3H_2O + 2K^+$$

Textural relations indicate that pyrophyllite occurs as a retrograde alteration product of andalusite, and probably formed during waning contact alteration as follows:

$$\underset{\text{andalusite}}{Al_2SiO_5} + \underset{\text{quartz}}{3SiO_2} + H_2O = \underset{\text{pyrophyllite}}{Al_2Si_4O_{10}(OH)_2}$$

Chlorite was probably in part derived from the breakdown of igneous ferromagnesian silicates, but some formed at the expense of muscovite:

$$\underset{\text{muscovite}}{2KAl_3Si_3O_{10}(OH)_2} + \underset{\text{quartz}}{3SiO_2} + 24H_2O + 15Fe^{2+} = \underset{\text{Fe-chlorite}}{3Fe_5Al_2Si_3O_{10}(OH)_8} + 28H^+ + 2K^+$$

Chloritoid formation probably involved the late-stage breakdown of chlorite:

$$\underset{\text{Fe-chlorite}}{2Fe_5Al_2Si_3O_{10}(OH)_8} + 16H^+ = \underset{\text{Fe-chloritoid}}{Fe_2Al_4Si_2O_{10}(OH)_4} + \underset{\alpha\text{-quartz}}{4SiO_2} + 8Fe^{2+} + 14H_2O$$

The occurrence of andalusite within the prograde paragenesis indicates that the pressure during alteration was less than 4.2 - 4.5 kbar (Bohlen et al., 1991; Pattison, 1992). Minimum temperatures during prograde alteration are limited to greater than ~380 – 410 °C by the stability of biotite, and the absence of pyrophyllite within the prograde paragenesis (Hemley et al., 1980; Aggarwal and Nesbitt, 1987; Zhou et al., 1994). Maximum temperatures along the immediate Stentor pluton contact are only loosely constrained to less than 600°C at 2 kbar or 680°C at 4.5 kbar by the stability of quartz + muscovite (Chatterjee and Johannes, 1974), and the absence of sillimanite. Metamorphic studies elsewhere along the northern flank of the BGB indicate that rocks in the contact aureole of the Nelspruit batholith attained the amphibolite facies (Anhaeusser, 1972), with temperatures of 520-580°C estimated for syn-metamorphic gold mineralization at the New Consort Gold Mines (Tomkinson and Lombard, 1990). Maximum temperatures away from the immediate Stentor pluton contact can be constrained to less than 460–530°C by the stability of chloritoid (Ganguly, 1969), but are subject to chemical and O_2 fugacity provisos.

Quartz-muscovite schists along the Stentor pluton contact contain quartz ± tourmaline veins, some exceeding 70 m in length, that generally lie within the S_2 foliation. The host rocks to these veins are commonly intensely silicified and tourmalinized. Some of the tourmaline-bearing veins are characterised by a crude banding consisting of alternating quartz- and dense green-black tourmaline-rich layers oriented subparallel to the vein margins. There is little doubt that these veins resulted from silica and boron metasomatism accompanying the intrusion of the Stentor pluton.

GEOCHEMISTRY

Sampling and Analytical Techniques

Chemical analyses of least-altered samples of quartz-muscovite, biotite-plagioclase and chloritic schist from the Bien Venue Formation in the Three Sisters area are presented in Appendix I (Tables 1-3), along with a series of chemical ratios. For comparative purposes, five samples of silicic metavolcanic rock and quartz-muscovite schist from the Theespruit Formation in the southwestern part of the BGB, and the Weergevonden greenstone remnant (Anhaeusser, 1980), were analysed to supplement two analyses reported by Glikson (1976). These data, together with the analyses from Glikson (1976), are provided in Appendix I (Table 4). Table 5 (also in Appendix I) shows analyses of dacitic metavolcaniclastic rocks (biotite-feldspar schists) from the Schoongezicht Formation. These specimens were collected from road-cuttings in the type-area of the Schoongezicht Formation in the closure of the Stolzburg syncline (Lowe and Byerly, 1999; Condie et al., 1970), and from exposures along the northern limb of the Eureka syncline at Ezzey's Pass and south-southeast of New Consort Gold Mine (Anhaeusser, 1976). Detailed sample descriptions and locations are given in Kohler (1994).

Major element data were obtained by standard X-ray fluorescence spectrometry (XRF) analysis of fused disks following the method of Norrish and Hutton (1969). All iron is reported as $Fe_2O_3^{total}$. H_2O^- and H_2O^+ were determined gravimetrically and by infrared adsorption on Leco RMC-100 and RC-412 moisture analysers. CO_2 was determined using a Leco CS-244 infrared absorption spectrometer. Routine precision of the major element analyses is 1-5 % at reasonable concentration levels.

Trace element (Ba, Rb, Sr, Y, Nb, Zr, Ga, Zn, Cu, Ni, Pb, V and Cr) concentrations were also determined by XRF on pressed briquettes. Detection limits are 5-10 ppm for Ba, 2-5 ppm for Rb, Sr, Pb, Y, Nb, Zr, V, Cr and Cu, and 1 ppm for Ga, Zn and Ni. Analytical uncertainty is estimated at less than 10-15% for Nb and Cr, and less than 5-10% for the remaining trace elements.

Abundances of the rare-earth elements (REEs), Cs, U, Th, Hf, Ta, Co and Sc were determined by instrumental neutron activation analysis (INAA), following Fesq et al. (1973) and Erasmus et al. (1977), using multichannel Ge and Ge-(Li) detectors housed at the Schonland Research Centre for Nuclear Science, Johannesburg. Concentrations of Na_2O in the quartz-muscovite schists of the Bien Venue Formation are below the detection limit of the XRF methods employed, and were also determined by INAA. Primitive-mantle and C1 chondrite-normalized diagrams and values (denoted by the subscript $_{cn}$) use factors from Sun and McDonough (1989). Averaged values are denoted by the superscript ^{av}.

Chemical Mobility and Immobile Element Residual Enrichment

Samples showing intense deformation and alteration were avoided for this study, so that the analyses listed reflect, as closely as possible, primary compositions. Nonetheless, the interpretation of the chemical data is constrained by the mobility of certain elements during low- to medium-grade metamorphism and alteration. Under these conditions, the least mobile elements are likely to have been the high field-strength elements (HFSEs: Ti, Y, Nb, Zr, Hf, Ta), the REEs (possibly with the exception of Eu), Al, Th, P and some transition metals (V, Cr, Sc, Ni), whereas other major elements (including Si, Fe, Mg, Ca, Na and K) and the lithophile trace elements (Ba, Rb, Sr, Cs) may have experienced substantial mobility (Finlow-Bates and Stumpfl, 1981; MacLean and Kranidiotis, 1987; Whitford et al., 1989; Vance and Condie, 1987; MacLean and Barrett, 1993; Cullers et al., 1993).

There are a number of tests for element mobility/immobility based on simple inter-element correlations (e.g., Finlow-Bates and Stumpfl, 1981; Maclean and Kranidiotis, 1987; MacLean, 1990; MacLean and Barrett, 1993). Kohler (1994) demonstrated that lithophile trace element concentrations in the quartz-muscovite schists vary systematically with K and Na, consistent with control by muscovite, and paragonite component of muscovite, respectively. The HFSEs and most other alteration insensitive elements, on the other hand, do not show any systematic variations with lithophile element concentrations. Nonetheless, binary plots utilising these immobile elements seldom yield well-defined linear alteration arrays, reflecting primary geochemical heterogeneities in the precursor suite (Kohler, 1994).

It is important to note that despite assumed immobility, concentrations of the alteration insensitive elements are unlikely to reflect original values due to the effects of residual enrichment accompanying volume change during schistosity development. Although it is not possible to quantify the volume loss accompanying deformation of the Bien Venue Formation rocks, owing to a lack of suitable unaltered material and strain markers, detailed studies on cleaved metasediments in younger terranes have indicated volume losses of between 5-50% (e.g., Tan et al., 1995; Goldstein et al., 1995). Accordingly, the measured HFSE and REE concentrations are regarded as maxima. However, accepting that the immobile elements in any given sample will have undergone the same degree of residual enrichment, it follows that ratios of alteration insensitive elements, and the shapes and slopes of chondrite- and primordial-mantle normalized plots, reflect those of the precursor suite, despite vertical migration with respect to the y axis.

Quartz-muscovite Schists

Utilising the Zr/TiO_2 versus Nb/Y classification of Winchester and Floyd (1977), the quartz-muscovite schists plot as dacite-rhyodacite, with overlap into the andesite and trachyandesite fields (Fig. 7). SiO_2 ranges from 63 to 80 wt%, but in most cases exceeds 72 wt%; samples containing abundant quartz porphyroclasts (BVR3, BVR10, BVR18) characteristically possess the highest SiO_2 contents. The schists are poor in the ferromagnesian elements, with $Fe_2O_3^{total}$+MnO+MgO ≤5 wt% (Fig. 8a). Al_2O_3 varies mostly exceeds 15 wt%, with values as high as 19 wt% (Fig. 8b). K_2O spans 1.4 to 6.2 wt%; but Na_2O concentrations in the majority of samples are exceptionally low (<0.45 wt%); the higher Na_2O value of 3.8 wt% recorded for sample BVR15 reflects the presence of relic plagioclase (Fig. 9a). CaO contents are also usually very low (<0.35 wt%); the elevated CaO values of BVR15 (1.2 wt%) and BVR16 (3.6 wt%) are attributed to plagioclase and secondary calcite, respectively. The marked depletion of Na^+ and Ca^{2+} relative to K^+ during alteration reflects the breakdown of plagioclase to muscovite, and is manifest in the high K_2O/Na_2O (5.4-21) and K_2O/CaO (1.4-210, but mostly >7) ratios recorded for the feldspar-free samples. By contrast, BVR15 displays K_2O/Na_2O=0.44 and K_2O/CaO=1.7. The hydrolysis of plagioclase also led to the marked depletion of Sr in most samples (<50 ppm), whereas BVR15 contains 120 ppm (Fig. 9b). Consequently, Sr/Y values for the majority of samples are less than 2. Contents of Ba and Rb range, respectively, from 96 to 299 ppm and 35 to 124 ppm (Fig. 9c). Ti/Zr values span 13-27 (Fig. 10a).

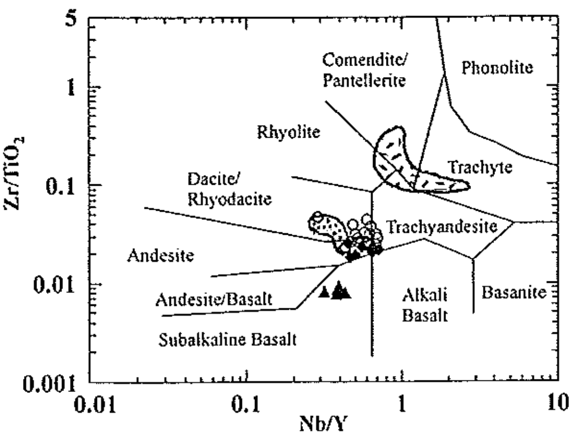

Figure 7: Classification plot of Zr/TiO_2 versus Nb/Y (after Winchester and Floyd, 1977) for the schistose metavolcaniclastic rocks of the Bien Venue Formation. Symbols: open circles – quartz-muscovite schists; diamonds – biotite-plagioclase schists; triangles – chlorite schists. Also shown are the compositions of metavolcanic rocks from the Theespruit (random dashes) and Schoongezicht Formations (grey stipple).

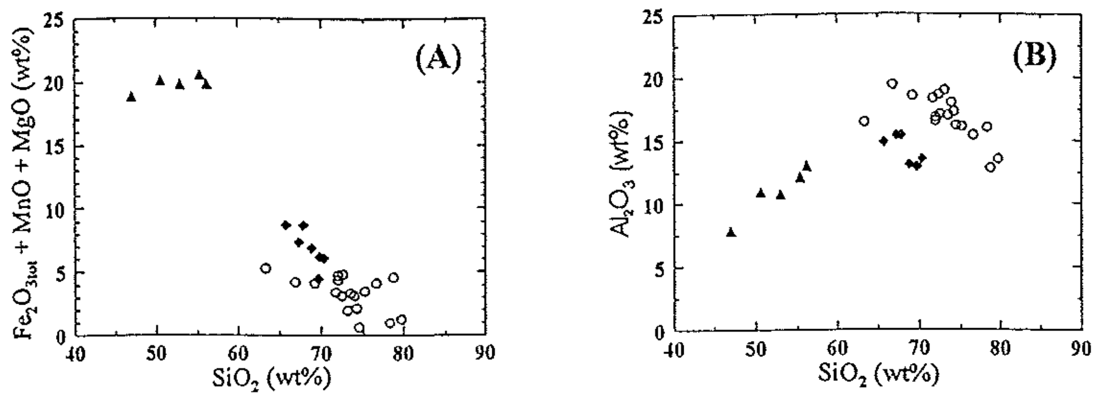

Figure 8: Binary plots of SiO_2 versus (a) $Fe_2O_3^{total}$ + MnO + MgO, and (b) Al_2O_3 for silicic and basic metavolcaniclastic lithologies of the Bien Venue Formation.Symbols as in Figure1.

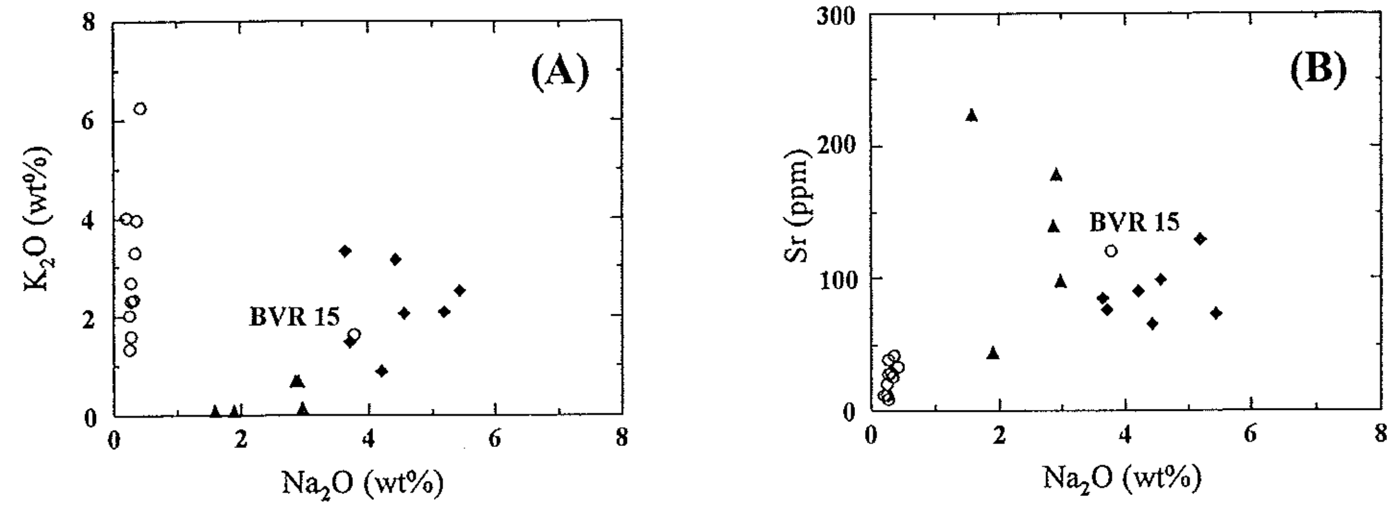

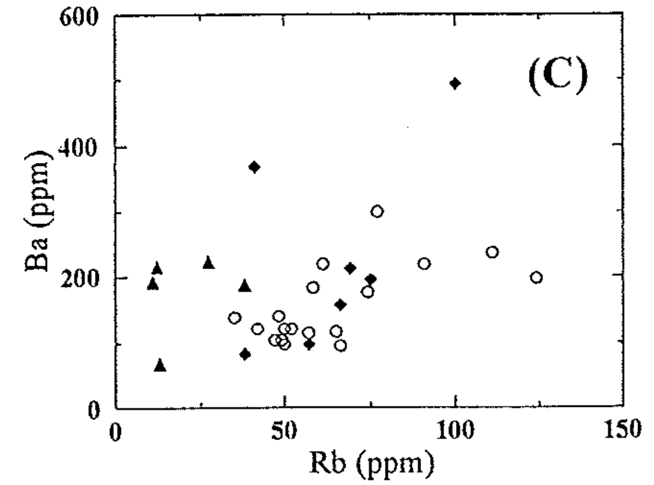

Figure 9: Plots of : (a) K_2O versus Na_2O, (b) Sr versus Na_2O, and (c) Ba versus Rb for the Bien Venue schists. Symbols as in Figure7.

The rocks are characterised by moderate enrichment of the LREE relative to the HREE (La_{cn}=70-140; Yb_{cn}=7.1-21; $[La/Yb]_{cn}$=6.8-12; $[Ce/Yb]_{cn}$=5.5-9.7), near flat HREE profiles ($[Tb/Yb]_{cn}$=1.0-2.0), with no, or only small, negative Eu anomalies (Eu/Eu*=0.72-1.03; Fig. 11a). A primitive-mantle normalized immobile element plot shows depletion of Ta-Nb relative

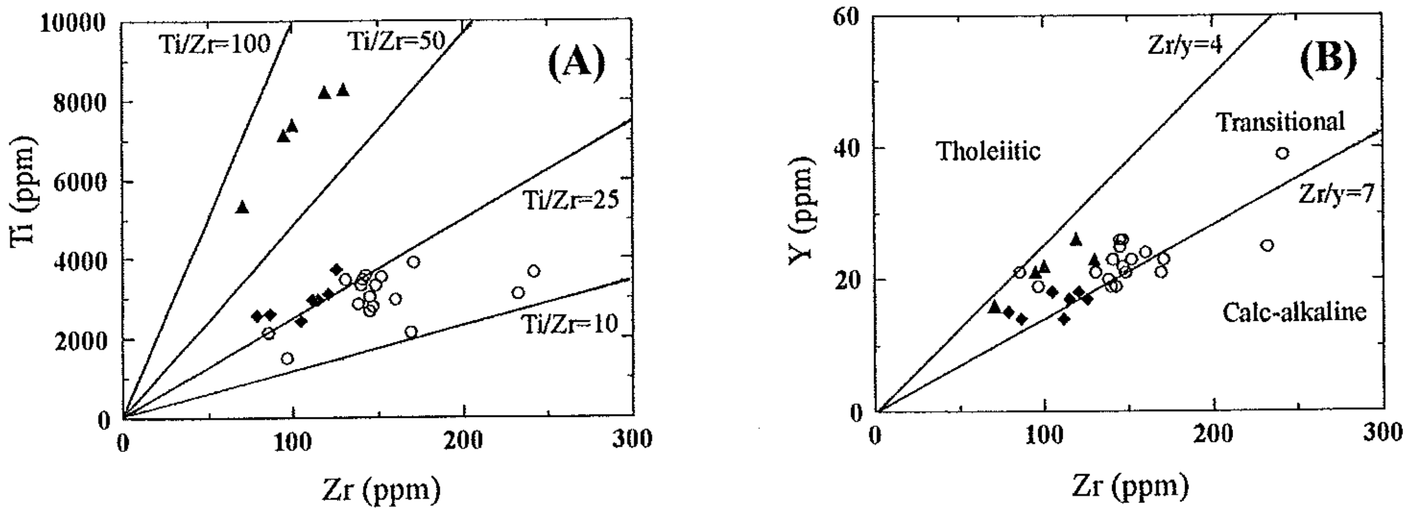

Figure 10: Plots of Zr versus (a) Ti, and (b) Y for the schists of the Bien Venue Formation. Symbols as in Figure 7. Zr/Y field boundaries after Barrett and MacLean (1997).

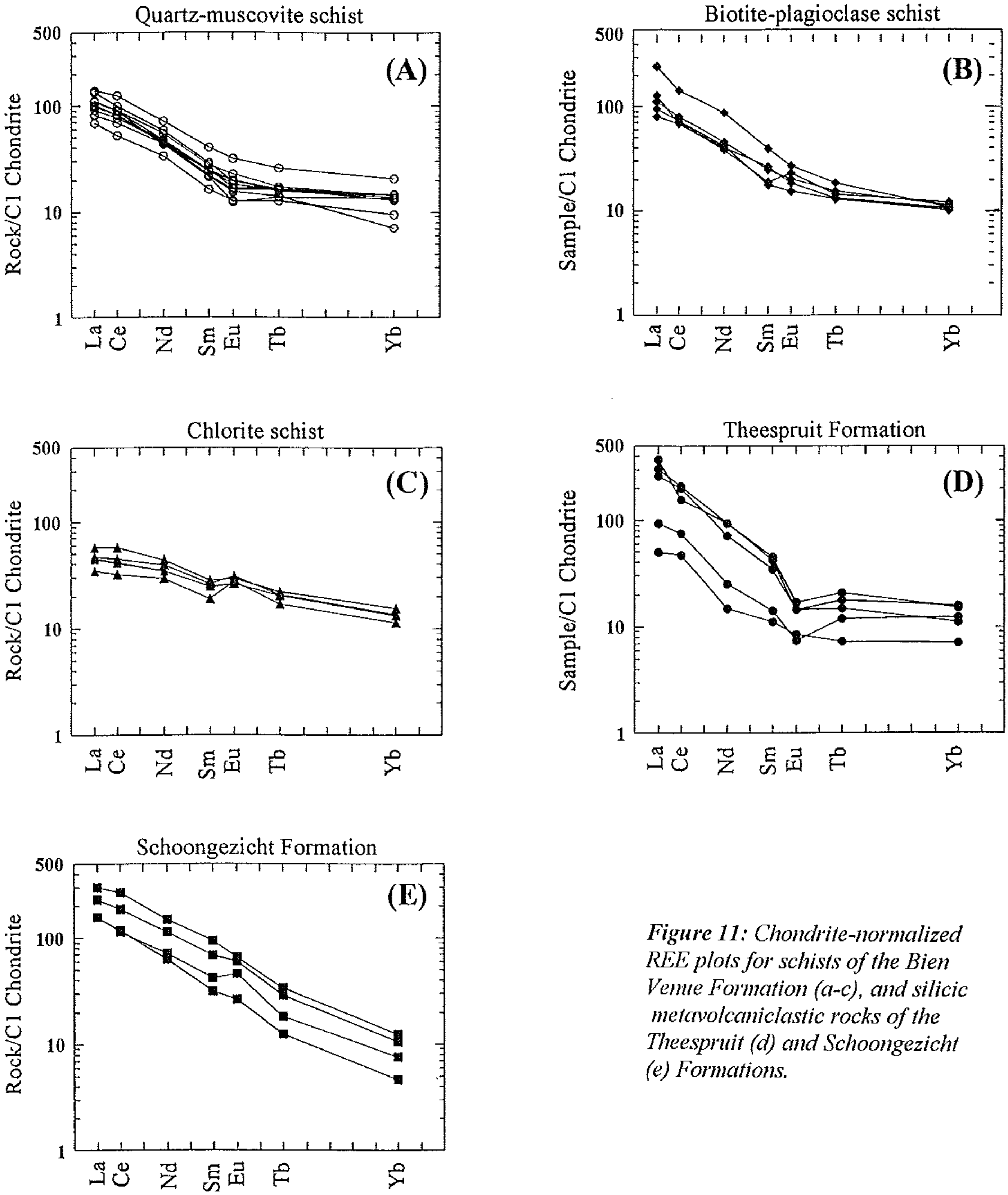

***Figure 11:** Chondrite-normalized REE plots for schists of the Bien Venue Formation (a-c), and silicic metavolcaniclastic rocks of the Theespruit (d) and Schoongezicht (e) Formations.*

to Th-U and La-Ce, as well as prominent troughs at P (BVR6 excluded) and Ti, consistent with a subduction-associated petrogenesis (Fig. 12a; Hildreth and Moorbath, 1988; Hawkesworth et al., 1993; Brenan et al., 1994). These profiles, coupled with low-to-moderate incompatible element concentrations (Y mostly <26 ppm; Nb <20 ppm; Zr <250 ppm; Hf <5.5 ppm; Ta <1.2 ppm; Th <7 ppm) and selected interelement ratios (e.g., Nb/Y=0.29-0.70;

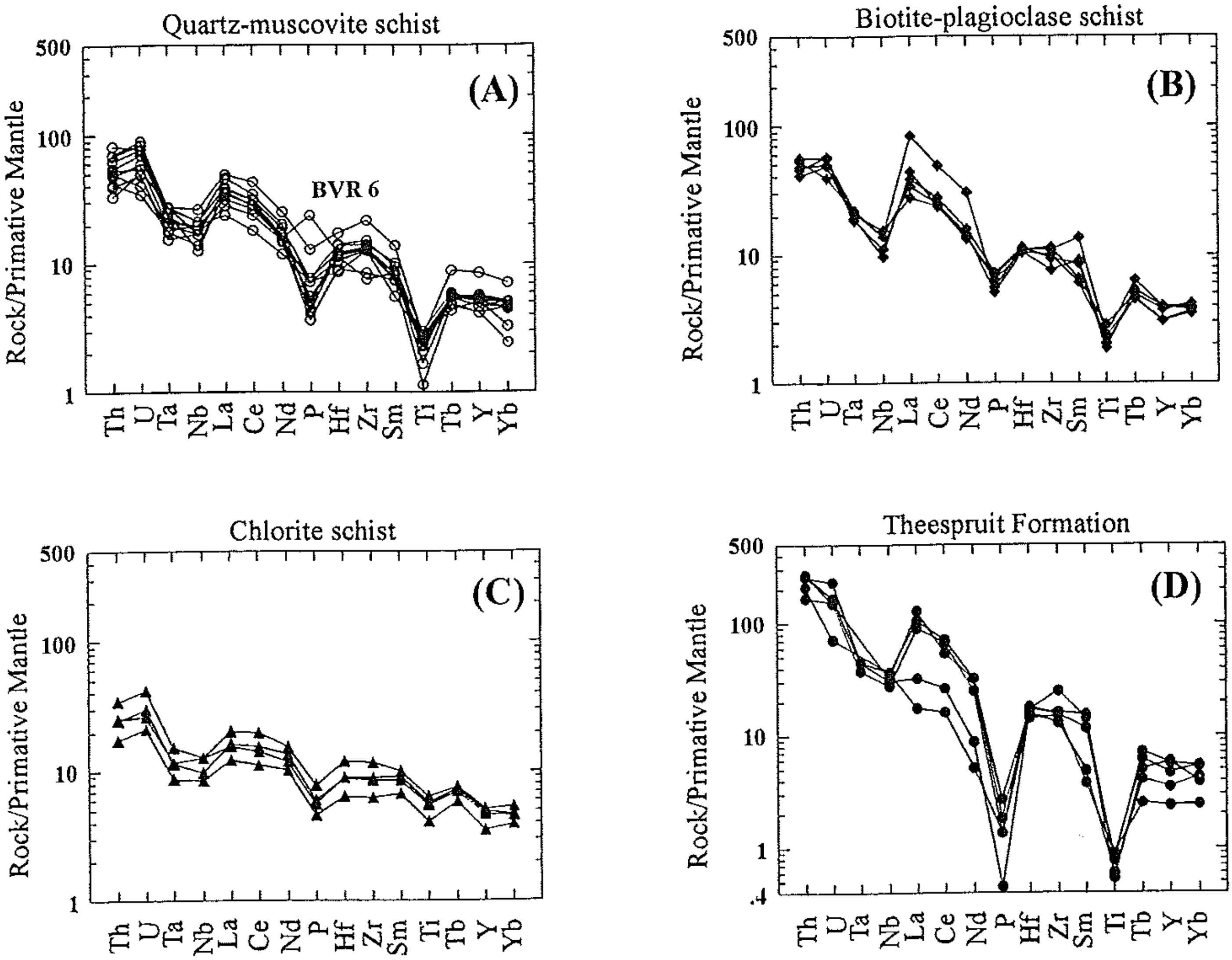

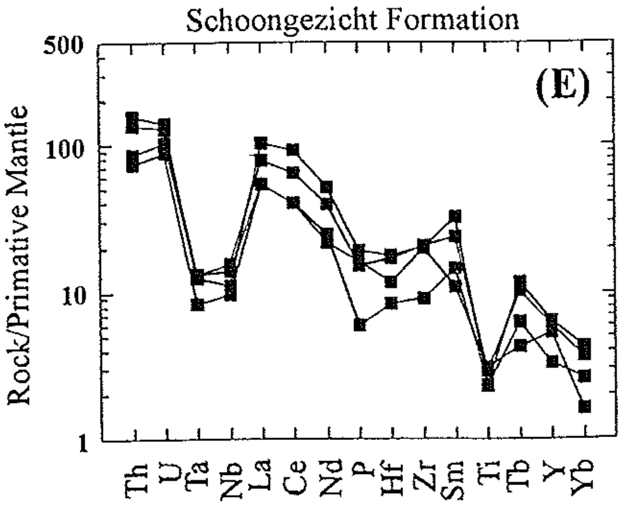

Figure 12: Primitive-mantle normalized immobile multi-element plots for schists of the Bien Venue Formation (a-c), and samples from the Theespruit (d) and Schoongezicht Formations (e).

Th/Yb=1.4-3.0; Zr/Nb mostly 8-15), suggest that the schists represent a calc-alkaline arc suite, although moderate Zr/Y (4.0-9.3) values suggest some transitional affinities (Fig. 10b; see Pearce, 1983; Pearce et al., 1984; Condie, 1986; Harris et al., 1986; Barrett and MacLean, 1997). The rocks are similar to post-Archaean subduction-related granitoids, which typically have $[La/Yb]_{cn}<25$ at $Yb_{cn}>5$, and Y=15-50 ppm (Martin, 1986, 1993). The rocks are also

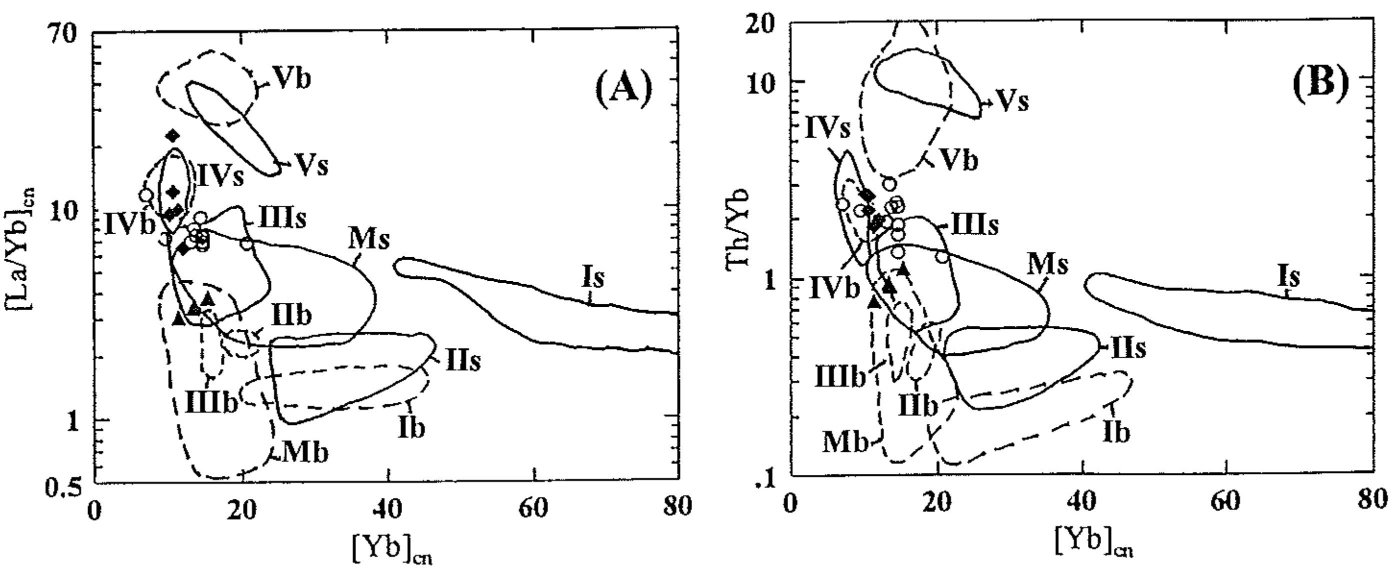

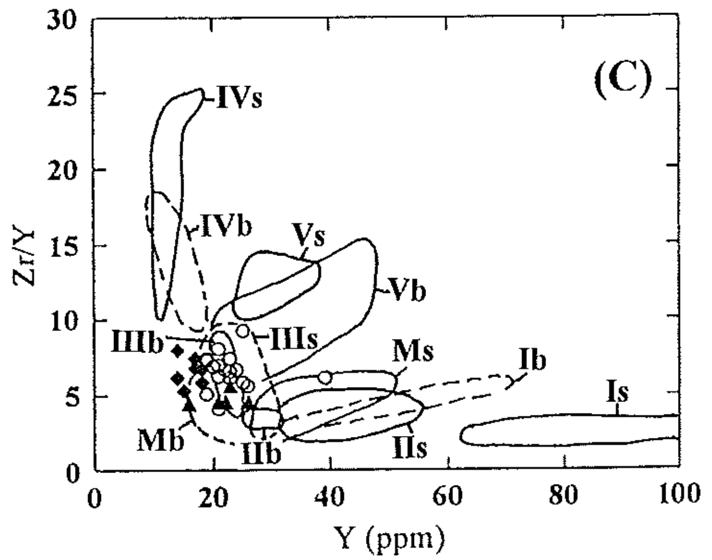

Figure 13: Binary geochemical comparison diagrams of the Bien Venue Formation schists with the major groups of VHMS-bearing and barren, basic and silicic metavolcanic sequences defined by Barrie et al. (1993) for the Abitibi subprovince, Canada, based on : (a) $[La/Yb]_{cn}$ – Yb_{cn}, (b) Th/Yb - Yb_{cn}; and (c) Zr/Y – Y systematics. Symbols as in Figure 7. Roman numerals refer to groups listed in Appendix I, Table 6; subscript letters denote silicic ($_s$) or basic ($_b$) metavolcanic suites. M shows the field for metavolcanics of the Misema Group, Canada.

comparable with the Group III (Selbaie) and Type-FI silicic-intermediate metavolcanic sequences defined by Barrie et al. (1993) and Lesher et al. (1986), respectively, for the Superior Province of Canada (Fig. 13a-c). Barrie et al. (1993) demonstrated that Group III rocks are geochemically similar to calc-alkaline volcanics erupted in Phanerozoic continental margin arc settings (Appendix I, Table 6).

The high Al_2O_3 contents of the schists fall within the range of values recorded for Archaean high-Al TTGs and Cenozoic adakite sequences, which have Al_2O_3 between 13-20 wt% (Drummond et al., 1996). However, the rocks do not display the extreme REE fractionation ($[La/Yb]_{cn}^{av}$=31; $[Ce/Yb]_{cn}^{av}$=27) and low Yb_{cn}^{av} (2.2) and Y^{av} (4 ppm) values of these suites (values from Feng and Kerrich, 1992; Feng et al., 1993). The schists also differ from Archaean low-Al TTGs which are generally characterised by less fractionated REE profiles ($[La/Yb]_{cn}^{av}$=3.3; $[Ce/Yb]_{cn}^{av}$=3.1) at higher Yb_{cn}^{av} (22) and Y^{av}(55 ppm;).

Compared with the silicic rocks of the Theespruit Formation, the quartz-muscovite schists generally have lower Na_2O, Ba and Nb, but are enriched in Al_2O_3, TiO_2 and V (Appendix I, Tables 1 and 4). Moreover, the Theespruit rocks are characterised by distinctly higher Nb/Y (0.73-2.4) values, more akin to modern alkaline associations (Fig. 7). Presented in Figure 14 are a series of ternary discrimination diagrams, two of which are based on elements of low mobility during alteration, highlighting some of these geochemical differences. Samples from the Theespruit Formation also exhibit a greater spread to higher La_{cn} (51-371), but similar Yb_{cn} (7.1-15.8), resulting in some steeper patterns with $[La/Yb]_{cn} = 7.2$-33.2 (Fig. 11d). The Theespruit samples are also typically characterised by moderate relative Eu depletion ($Eu/Eu^* \cong 0.58$; G34 excluded). A primitive-mantle plot shows higher relative abundances at Th and U than for the Bien Venue Formation schists, similar negative anomalies at Ta-Nb, but more pronounced troughs at P and Ti (Fig. 12d).

Figure 14: Ternary discrimination diagrams highlighting some geochemical differences between quartz - muscovite schists of the Bien Venue Formation (open circles) and felsic metavolcanic rocks of the Theespruit Formation (closed circles).

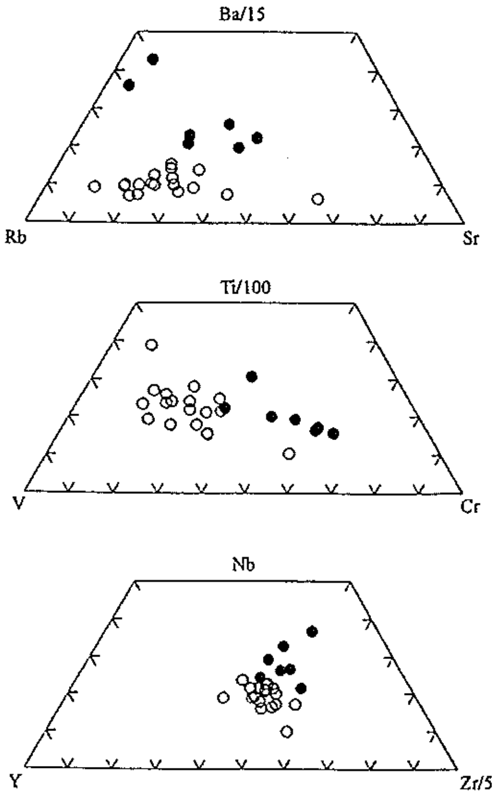

Biotite-plagioclase Schists

On the Zr/TiO_2 versus Nb/Y classification diagram, the biotite-plagioclase schists plot in the andesite field, although overall, the geochemical data suggest that the rocks were probably derived from a dacitic precursor. Concentrations of SiO_2 and $Fe_2O_3^{total}$ range from 66 to 70 wt% and 3.0 to 4.5 wt%, respectively. Al_2O_3 is consistently below 16 wt%. Two less evolved samples (BVD3 and BVD7) have up to 4.3 wt% MgO.

Compared with the quartz-muscovite schists, these rocks are generally distinguished by higher Na_2O (3.6-5.4 wt %), Sr (66-129 ppm) and CaO (0.9-2.8 wt%), reflecting the ubiquitous presence of plagioclase and calcite (Fig. 9a-b). Contents of Rb, Ba and K_2O (0.9-3.3 wt%) are mostly similar, leading to lower K_2O/Na_2O (0.21-0.91) and K_2O/CaO (0.59-3.6) ratios.

Despite their ferromagnesian-rich mineralogy, the rocks exhibit similar concentrations of TiO_2 to the quartz-muscovite schists, but are on average depleted in Zr (106 versus 151 ppm) and Y (16 versus 23 ppm), with comparable to higher Ti/Zr (23-33) and Zr/Y (5.3-7.9), and significantly higher Sr/Y (3.9-7.6).

REE plots show moderately fractionated calc-alkaline profiles ($[La/Yb]_{cn}$=6.6-22.6; $[Ce/Yb]_{cn}$=5.7-13.1) with flat HREE traces ($[Tb/Yb]_{cn}$=1.2-1.7) at similar total REE contents to the quartz-muscovite schists (La_{cn}=80-243; Yb_{cn}=10-12), and no, or slight positive, Eu anomalies (Eu/Eu*=0.99-1.39; Fig. 11b). These profiles show many of the features of post-Archaean arc-related granitoid suites (Martin, 1986, 1993). A multi-element diagram shows strong normalized relative depletions at Nb-Ta, P and Ti, similar to sequences from convergent margin settings (Fig. 12b). In terms of $[La/Yb]_{cn}$, Th/Yb and Zr/Y values, the biotite-plagioclase schists are comparable with both the Group III and Group IV associations defined by Barrie et al. (1993). The rocks differ from Archaean high-Al TTGs in terms of lower $[La/Yb]_{cn}$ and $[Ce/Yb]_{cn}$, but higher Yb_{cn} and Y, and from low-Al TTGs by greater degree of REE fractionation, and lower Yb_{cn} and Y.

The biotite-plagioclase schists are similar in major element geochemistry, despite slightly higher SiO_2 contents, to the calc-alkaline dacitic volcaniclastic rocks of the Schoongezicht Formation. However, notable differences are evident in the concentrations of some trace elements, particularly Ba and Sr, and to a lesser degree Zr, Rb and Th, which are typically enriched in the Schoongezicht samples (Appendix I, Tables 2 and 5). The two suites also differ markedly in the values of selected immobile trace element ratios, for example Zr/Nb (10-13 versus 14-29) and La/Ta (22-64 versus 69-140), the latter in part due to more pronounced relative depletion at Ta-Nb for the Schoongezicht rocks (Fig. 12e). Furthermore, the Schoongezicht volcaniclastics are typically enriched in the LREE and the MREE relative to the Bien Venue schists, but have similar or lower HREE contents, and are consequently distinguished by higher $[La/Yb]_{cn}$ (21-34) and $[Tb/Yb]_{cn}$ (2.4-2.7), but similar Eu/Eu* (1.19-1.67; Fig. 11e).

Chlorite Schists

In Figure 7, the chlorite schists plot in the field of sub-alkaline basalts. Major element abundances also point to a basaltic or basaltic andesite protolith, with SiO_2 in the range 47-56 wt%, $Fe_2O_3^{total}$ between 13-18 wt% and moderate MgO contents (2.8–5.5 wt%). High CO_2 and low K_2O contents stem from alteration processes.

The schists show slightly fractionated LREE to HREE patterns ($[La/Yb]n$ = 3.1-3.8) with small positive Eu anomalies (Eu/Eu* = 1.19-1.53; Fig. 11c). These features, coupled with Zr/Y = 4.4-5.7 and Th/Yb = 0.76-1.12, indicate an affinity transitional between tholeiitic and calc-alkaline (see Pearce, 1983; Barrett and MacLean, 1997). Compared to normal-type mid-ocean ridge basalt (N-MORB; Sun and McDonough, 1989), the schists are strongly enriched in U and Th (9-24 times N-MORB), moderately enriched in Nb, Ta and LREEs (1.9-5.5) and depleted in Y and HREEs (0.6-0.9). The rocks are comparable with both the Group III Selbaie calc-alkalic volcanic sequences, as well as the tholeiitic to calc-alkaline rocks of the Misema Group in the Abitibi subprovince of Canada. A primitive-mantle-normalized diagram shows a weak subduction-related signature with troughs at Ta-Nb, P and Ti (Fig. 11c). Low abundances of Cr (less than detection limit to 66 ppm) and Ni (15-78 ppm) are accompanied by elevated LILE/LREE and LILE/HFSE values (e.g., Ba/La = 4.9-23; Ba/Zr = 0.5-2.7, but generally > 1.9), similar to modern arc basaltic suites (see Ewart, 1982; Pearce, 1982; Arculus and Powell, 1986; Fryer et al., 1990; Hawkesworth et al., 1993). However, Ti/V values (30-52) are higher than those recorded in modern subduction-related suites, and are more typical of oceanic basalts extruded at mid-ocean ridge and back-arc spreading centres (see Shervais, 1982; Fryer et al., 1990). Nonetheless, the schists also possess moderately high Th/Nb (0.24-0.33) and Th/La (0.18-0.21) values, suggesting possible contamination by upper crustal materials (see Vearncombe and Kerrich, 1999). Furthermore, in terms of Ta/Yb (0.19-0.14), Nb/Yb (3-4) and Zr/Y ratios, the rocks are identical to basalts erupted at active continental margins (see Pearce, 1983; Pearce and Peate, 1995).

DISCUSSION

Stratigraphic Implications and Geochronology

Silicic and basic schists in the Three Sisters area were previously included with the Theespruit Formation of the lower Onverwacht Group, but are here considered to be a separate lithostratigraphic unit, the Bien Venue Formation. Structural relations indicate that the Bien Venue Formation is the uppermost unit of the Fig Tree Group in the northeastern sector of the BGB.

Although there are a number of obvious similarities between the Theespruit and Bien Venue Formations, notably the presence of aluminous quartz-muscovite schist, there are also important lithologic differences. Whereas the Theespruit Formation is made up largely of basic and ultrabasic rocks, with subordinate intercalations of silicic schist (Viljoen, M.J. and Viljoen, 1969a,b; Viljoen et al., 1969; Lowe and Byerly, 1999), the Bien Venue Formation is composed almost entirely of quartz-muscovite schist, and only minor basic schist. Geochemical work has also revealed subtle, but distinctive differences in the major and trace element compositions of silicic rocks from these formations, indicating that they belong to separate suites. In addition, at several localities, the Bien Venue Formation contains biotite-plagioclase schists, which have not been reported from the Theespruit Formation. The biotite-plagioclase schists were derived from dacitic precursors comparable to the plagioclase-phyric volcaniclastic rocks making up much of the Schoongezicht Formation (Condie et al., 1970; Anhaeusser, 1976; Lowe and Byerly, 1999). The Schoongezicht volcaniclastic sequences mark the top of the Fig Tree Group in the northwest and central parts of the BGB. However, despite similarities in apparent stratigraphic position, significant lithologic, geochemical and age differences (see below) indicate that the Bien Venue and Schoongezicht Formations are also separate units.

The new interpretation is supported by radiometric age determinations. Kröner et al. (1991) reported a zircon Pb-Pb evaporation age of 3259 ± 5 Ma for a sample of quartz-muscovite schist collected near the Bien Venue massive sulphide deposit. This age is within error of the single zircon U-Pb conventional age of 3256 ± 1 Ma (2J) obtained by Kohler (1994) from a sample collected near the stratigraphic top of the volcaniclastic pile east-northeast of Three Sisters. The latter age is regarded as the best age estimate of the Bien Venue Formation, and is some ~290–200 Ma younger than the most recent age determinations on rocks correlated with the Theespruit Formation (3548 ± 1.3 Ma to 3453 ± 6 Ma: Armstrong et al., 1990; Kröner et al., 1991) in the southwestern part of the BGB. Further, the Bien Venue schists are ~30 Ma older than the rocks of the Schoongezicht Formation (3226 ± 1 Ma to 3222 +10/-4 Ma: Kröner et al., 1991; Kamo and Davis, 1994), precluding direct correlation with the latter unit.

The available isotopic data suggest that the Bien Venue Formation may be a temporal correlative of the Auber Villiers Formation, which has been dated at 3256 ± 4 Ma and 3253 ± 3 Ma (Kröner et al., 1991; Byerly et al., 1996). The latter formation is exposed south of the Inyoka zone, and is composed largely of proximal plagioclase-phyric dacitic epiclastic sequences (Lowe and Byerly, 1999). The Bien Venue rocks may, in part, also be age correlatives of syndepositional quartz-phyric dacitic volcaniclastic units within the Mapepe Formation (Nocita and Lowe, 1990; Lowe and Nocita, 1999), which have yielded single-crystal zircon ages of 3258 ± 3 Ma (Byerly et al., 1996), 3243 ± 4 Ma and 3227 ± 4 Ma (Kröner et al., 1991). Further studies are required to test these stratigraphic correlations.

The Bien Venue Formation is ~30-40 Ma older than the Kaap Valley tonalite (3229 ± 5 Ma to 3226 ± 14 Ma; Tegtmeyer and Kröner, 1987; Armstrong et al., 1990; Kamo and Davis, 1994) and the Nelshoogte trondhjemite (3213 ± 4 Ma; Layer et al., 1998). These data indicate that Bien Venue strata are not the coeval effusive equivalents of TTG plutonism along the northern flank of the BGB, as has been proposed for the dacitic volcaniclastic rocks of Schoongezicht Formation (de Wit et al., 1987a; Kröner et al., 1991; Kamo and Davis, 1994; Lowe, 1999).

Depositional Setting

Metamorphism and strong deformation have destroyed most of the primary textural characteristics of the Bien Venue strata and, hence, any discussion pertaining to their depositional setting cannot be definitive. However, despite these limitations, some broad interpretations concerning the environment of deposition can be made on the basis of available field evidence.

Quartz insets have been widely documented in quartz-muscovite schists in many ancient terranes. Studies have shown that the insets are inverted ß-quartz phenocrysts or pyrogenic crystals (Frater, 1983; Vernon, 1986; Williams and Burr, 1994). The feldspar porphyroclasts in the biotite-plagioclase schists are similarly interpreted as relic phenocrysts or pyrogenic grains. The evidence thus indicates that the porphyroclastic schists were derived from crystal-rich protoliths. According to Cas and Wright (1987), the production of crystal-rich volcanic-volcaniclastic rocks can be attributed to: (1) the eruption of highly crystallised magmas from shallow-level magma chambers; and/or (2) syn- to post-eruptive physical crystal fractionation mechanisms that lead to the concentration of resistant grains. The irregular embayments that characterise the majority of quartz, and some of the plagioclase porphyroclasts can be attributed to magmatic resorption prior to eruption (Vernon, 1986). The rounding of the corners of some porphyroclasts may reflect epiclastic reworking, but may also have resulted from pre-eruptive reaction with magma (Cas and Wright, 1987). The possibility that some of the porphyroclastic schists represent near-surface intrusive rocks also cannot be discounted.

Schistose conglomeratic units containing clasts of recrystallised chert or metavolcanic detritus indicate that the volcanic pile was subjected to post-eruptive reworking. Cas and Wright (1987) demonstrated that conglomerates in volcanic terranes form in alluvial or near-shore settings, but can also be the product of subaqueous mass flow processes. The degree of rounding of some clasts suggests that these were subjected to vigorous fluvial and/or wave-related abrasion. The occurrence of conglomeratic units as an integral part of the volcanic-volcaniclastic succession, coupled with the absence of extraneous clasts composed of ultrabasic, basic or granitoid material, indicates that the volcaniclastic sediments were derived solely from the localised, penecontemporaneous reworking of the volcanic pile.

The laminated phyllite and slate intercalations reflect sedimentation under quiet, subaqueous conditions. The muscovite-rich mineralogy of these rocks, coupled with the presence of embayed quartz insets and the absence of basic-ultrabasic or granitoid fragments, once again suggests that the sediments were locally derived.

The chert units are similar to black-and-white banded cherts elsewhere in the BGB. These rocks may have originated via a number of processes, including the precipitation of primary silica, possibly associated with seafloor exhalative fluid discharge. However, there is also evidence that indicates that the cherts represent silicified argillaceous and volcaniclastic sediments. Studies on similar rocks elsewhere in the BGB have indicated that the silicification took place during, or soon after, deposition of the sediments in response to surface or near-surface hydrothermal activity (Lowe and Knauth, 1977; Lanier and Lowe, 1982; Paris et al., 1985; Paris, 1990). The origin of the dolomite units is uncertain, although they probably represent silicified calcareous sediments.

Field and stable-isotope studies of the Stentor barite deposit led Viljoen, R.P. and Viljoen (1969b) and Reimer (1980; personal communication 1991) to conclude that the mineralization formed in a low-energy submarine environment as a consequence of synvolcanic fumarolic exhalations. Similarly, despite intense recrystallization and possible remobilisation during deformation and metamorphism, preserved textural evidence indicates that the Bien Venue massive sulphide deposit also resulted from sea-floor exhalative activity, similar to the polymetallic massive sulphide deposits of the Kuroko district in Japan (Murphy, 1990; P. Harrison, personal communication 1991).

Considering the available evidence, it seems likely that the rocks of the Bien Venue Formation were deposited in a subaqueous environment. The probable exhalative origin of the Bien Venue massive sulphide deposit also allows some conclusions to be drawn regarding the palaeodepth (shallow or deep) of the environment of deposition. Fluid inclusion (Pisutha-Arnond and Ohmoto, 1983) and foraminiferal studies (Guber and Merrill, 1983) have shown that the Kuroko volcanic hosted massive sulphide (VHMS) deposits formed at water depths of at least 1800 m. Modern Kuroko-type analogues presently forming on the sea floor and genetically related to silicic submarine volcanism in arc – back-arc settings, have not been recorded at depths shallower than ~1200 m (Kimura et al., 1988; Urabe and Kusakabe, 1990; Fouquet et al., 1993; Wright et al., 1998; Lizasa et al., 1999).

From the above, it seems likely that the Bien Venue Formation strata were, at least partly, deposited in a deep-marine environment. In making this statement, we do not preclude the possibility that some of the schists were derived from shallow-water or possibly even subaerial deposits, as it is likely that the volcanic terrane was characterised by considerable relief. Also, as previously discussed, degree of rounding of some clasts indicates high-energy reworking by fluvial or littoral processes in shallow to emergent parts of the volcanic complex. However, the resedimentation of subaerial and shallow-water deposits into deep-water environments has been widely documented in both modern and ancient volcanic terranes (e.g., Ricketts et al., 1982; Dolozi and Ayres, 1991; Car and Ayres, 1991; Cas, 1992), and probably also took place during deposition of the Bien Venue Formation. Although speculative, a deep-water setting for some parts of the Bien Venue Formation conforms with the postulated depositional environment for the underlying Sheba and Belvue Road Formations in the northern BGB (Eriksson, 1980a,b; Jackson et al., 1987; Lowe and Byerly, 1999).

Geodynamic Setting

Geochemical, geophysical and theoretical investigations during the past two decades have provided extensive evidence for the operation of a plate tectonic regime during the Archaean (e.g., Sleep and Windley, 1982; Windley, 1993; Calvert et al., 1995; Jackson and Cruden, 1995; Layer et al., 1998). Although the nature of this process is still the subject of debate, there is a growing realisation that most Archaean geodynamic processes were probably fundamentally similar to those during the Phanerozoic, albeit with some geochemical differences (e.g., Card, 1990; Cassidy et al., 1991; Feng and Kerrich, 1992; Barley, 1993; Abbott et al., 1994; Jackson et al., 1994).

Most of the silicic-intermediate volcanic-TTG assemblages in the Barberton area appear to have formed in subduction-related magmatic arcs (de Wit et al., 1987a, 1992; Lowe, 1999). Recently, Lowe (1999) proposed that the Kaap Valley tonalite pluton was temporally associated rocks of the Schoongezicht Formation formed in an arc – back-arc setting overlying a south-dipping subduction zone along the northern margin of the BGB at about 3226 Ma. Volcaniclastic units within the Mapepe and Auber Villiers Formations were similarly interpreted by Lowe (1999) as distal and proximal sequences, respectively, related to subduction and arc volcanism between 3258 Ma and 3227 Ma.

Previous sections of this paper have shown that in terms of REE and immobile trace element patterns, rocks of the Bien Venue Formation show strong similarities with transitional- to calc-alkaline assemblages in modern continental arcs, as distinct from spreading ridge or intraplate hotspot and rifting-related suites. Specifically, low-to-moderate abundances of the HFSEs, coupled with troughs at Ta-Nb and Ti on normalized multi-element diagrams such as those presented in Figure 12, provide key evidence of a subduction-related petrogenesis (e.g., Briqueu et al., 1984; Saunders et al., 1987; Stolz et al., 1990; Van Bergen et al., 1992). Several hypotheses have been proposed to explain the depletion of Ta and Nb in arc magmas compared to highly incompatible elements such as Th, U and the LREEs, and Ti relative to the MREEs. These include: (1) retention by mantle peridotite during interactions with the ascending melts (Kelemen et al., 1993); and (2) retention by residual Ti-bearing phases such as rutile, perovskite or titanite during melt generation (Saunders et al., 1980; Brenan et al., 1994).

Martin (1986, 1993) and Condie (1989) demonstrated that there are significant geochemical differences between most Archaean and post-Archaean subduction-related suites reflecting a change in the dominant process of magma generation between these eras. These differences are largely attributed to the lower thermal state of most modern (i.e., Phanerozoic) subduction systems compared to Archaean analogues, brought about by a number of interrelated factors. These include: (1) a cooler mantle; (2) lower rates of oceanic crust production; (3) slower rates of convergence of the subducting and overriding plates; (4) an older mean age and, hence, lower temperature of the subducted oceanic lithosphere; and (5) steeper angles of subduction (McCulloch, 1993; Tarney and Jones, 1994, Abbott et al., 1994).

Archaean high-Al TTGs were probably emplaced in magmatic arcs, but are depleted in the HREEs and Y compared to most Phanerozoic arc suites (Martin, 1986, 1993; Feng and Kerrich, 1992). These depletions suggest that high-Al TTGs were derived from shallow-level partial melting of relatively hot and young, flat-subducted tholeiitic basalt slabs in equilibrium with a garnet + hornblende residuum (Arkani-Hamed and Jolly, 1989; McCulloch, 1993;

Drummond et al., 1996). Direct slab melting of immature oceanic crust is relatively uncommon in modern subduction zones, but has been recorded in a few unique settings, including the Aleutian arc, Alaska (adakite suite: Defant and Drummond, 1990; Drummond et al., 1996), and Baja California, Mexico (bajaite suite: Saunders et al., 1987).

Slab melting and garnet + hornblende fractionation do not appear to have played an important role in the generation of Archaean low-Al TTGs and the vast majority of Phanerozoic subduction-related magmas (Feng and Kerrich, 1992; Martin 1986, 1993). Instead, these rocks appear to have resulted from deeper-level, volatile-induced anatexis of the overlying mantle wedge in response to dehydration of more mature, steeply subducted oceanic crust, followed by low-pressure fractional crystallization of plagioclase + pyroxene (Hawkesworth et al., 1993; Sutcliffe et al., 1993; Pearce and Peate, 1995).

The overall geochemical similarity of the quartz-muscovite and biotite-oligoclase schists within the Bien Venue Formation to continental arc suites suggests that they too originated via fusion of upper mantle material containing a hydrous component derived from the dehydration of steep subducted oceanic lithosphere. Vearncombe and Kerrich (1999) demonstrated that while slab anatexis of shallow subducted crust was the dominant process of magma generation in convergent margin settings during the Archaean, some steep subduction and volatile-initiated mantle-wedge fusion may have commenced as early as 3.3 Ga. The results of the present study provide further evidence for the operation of Phanerozoic-style subduction-zone petrogenetic processes during the Early Archaean.

Geochemical Signature of VHMS Mineralization

Geochemical studies have shown that most economic Cu-Zn VHMS deposits are hosted by volcanic suites that exhibit distinctive geochemical affinities (Lesher et al., 1986; Dostal et al., 1992; Barrie et al., 1993; Vearncombe and Kerrich, 1999). Barrie et al. (1993) subdivided the silicic and basic metavolcanic sequences of the Abitibi greenstone terrane into five groups reflecting the presence or absence of VHMS mineralization, geochemical affinity, and inferred tectono-magmatic setting. Discrimination between these suites is based on REE-HFSE abundances, and Th/Yb and Zr/Y values (Appendix I, Table 6; Fig. 13). An earlier study by Lesher et al. (1986) also emphasised the importance of the associated Eu anomalies to distinguish ore-associated sequences from barren suites.

Volcanic sequences corresponding to Groups I and II host significant VHMS deposits typically having tholeiitic or transitional tholeiitic – calc-alkaline signatures, and are interpreted to have formed in intra-oceanic rift or rifted island arc settings, respectively. REE profiles for these suites are flat and display significant negative Eu anomalies, the latter reflecting plagioclase fractionation in cogenetic high-level magma reservoirs that provided the heat source for the mineralising hydrothermal fluids (Lesher et al., 1986). Group I and II volcanic sequences comprise about 20% by area of the Abitibi greenstone terrane, but host over 85% of the VHMS mineralization by tonnage, including the major deposits at Kidd Creek, Noranda, Matagami and Val d'Or. In contrast, barren volcanic suites (Groups IV and V) show similarities with calc-alkaline and alkaline arc magmas that have undergone limited crustal contamination, with steep normalized REE slopes and Eu/Eu* ≥1, indicating that the rocks did not undergo significant magma chamber fractionation.

Rocks of Group III are characterised by moderately steep REE trends and resemble modern calc-alkaline supra-subduction continental margin sequences. Group III rocks are only known to host economic Zn-Cu mineralization at only one location, Selbaie, and exhibit strong geochemical similarities with the barren volcanic rocks of the Misema Group northeast of Rouyn-Noranda. According to Larson and Hutchinson (1993), the Selbaie ores are atypical of VHMS base-metal deposits, containing only minor syngenetic, stratiform sulphide mineralization, with the bulk of the ore in structurally controlled, epigenetic veins, breccias and stockworks.

The quartz-muscovite and chlorite schists of the Bien Venue Formation exhibit $[La/Yb]_{cn}$ and Zr/Y values comparable with the Group III category of Barrie et al. (1993). The biotite-oligoclase schists classify as both Group III and IV in terms of $[La/Yb]_{cn}$, but possess Zr/Y values characteristic of Group III. All of the schist varieties show a tendency towards higher Th/Yb than for comparable Group III volcanic suites in Canada (Fig. 13b). Importantly, the Bien Venue rocks are mostly characterised by no, or moderately positive, Eu anomalies, with only a few samples showing weak negative anomalies, suggesting that the rocks did not undergo significant fractionation in a high-level chamber.

We have not chemically analysed samples of quartz-muscovite schist from the immediate vicinity of the Bien Venue massive sulphide deposit due to the extreme state of deformation and alteration of rocks in the core of the Bien Venue synform, which render suspect assumptions of element immobility. Nonetheless, we conclude that despite showing evidence of Kuroko-type exhalative activity, the available chemical data indicates that the rocks of the Bien Venue Formation are of a type not usually associated with major (i.e., >10 million tonnes ore) VHMS deposits in other Archaean terranes.

CONCLUSIONS

Regional mapping has identified a new lithostratigraphic unit, the Bien Venue Formation, at the top of the Fig Tree Group in the northeastern sector of the BGB (Kohler, 1994, 2000). The new formation consists principally of quartz-muscovite ± andalusite ± chlorite ± chloritoid ± pyrophyllite schists derived from a proximal sequence of quartz-phyric dacitic-to-rhyodacitic volcaniclastic rocks, along with subordinate banded chert, interbedded argillite, and biotite-plagioclase ± chlorite ± carbonate- and chlorite ± carbonate ± amphibole schists. Geochemical data suggest that the latter rocks represent plagioclase-phyric dacitic and basaltic or basaltic-andesite volcanic-volcaniclastic units, respectively.

Although the Bien Venue strata were previously considered to form part of the Theespruit Formation, lower Onverwacht Group, structural relations, supported by radiometric studies that have yielded ages of 3259 ± 5 Ma and 3256 ± 1 Ma, indicate that the rocks are considerably younger than units of the lower Onverwacht Group. The Bien Venue Formation is also some 30 Ma older than the Schoongezicht Formation, the uppermost unit of the Fig Tree Group in the northwestern BGB. The rocks may be temporal equivalents of sequences within the Auber Villiers Formation, and possibly also sections of the Mapepe Formation, both of which belong to the southern facies of the Fig Tree Group (Nocita and Lowe, 1990; Lowe and Byerly; 1999; Lowe and Nocita, 1999).

Severe deformation and metamorphic alteration of the rock sequences have hampered interpretation of the environment of deposition during accumulation of the Bien Venue

Formation. Nonetheless, available textural evidence and rock associations suggest that the sequence was deposited in a subaqueous environment. Some preserved textures suggest reworking of parts of the volcanic-volcaniclastic pile in a high-energy shallow-water environment. However, the sequence also contains the Bien Venue VHMS deposit which shows similarities with Kuroko-type massive sulphide deposits currently forming in submerged arc and rifted back-arc settings at depths of >1km. Accordingly, we suggest that parts of the Bien Venue Formation, like those of the underlying Sheba and Belvue Road Formations of the northern Fig Tree facies, may have been deposited in a deep-water environment.

Rocks of the Bien Venue Formation exhibit a spectrum of compositions related in part to original igneous compositions, and in part to secondary deformation and alteration phenomena at moderate temperatures and pressures. Fabric and structural relations in the area north of Three Sisters suggest that most of this deformation and alteration accompanied the intrusion of the Stentor pluton at ca 3100 Ma. Microtextural relations indicate that mineralogical transformations during alteration of the quartz-muscovite schists were dominated by the hydrolysis of primary plagioclase and K-feldspar to muscovite, followed by the partial breakdown of muscovite to chlorite and andalusite, which shows retrograde replacement by pyrophyllite. Chloritoid probably formed by the hydrolysis of chlorite.

The quartz-muscovite schists are typically characterised by high SiO_2 and Al_2O_3, but extremely low Na_2O and Sr contents contributed to the destruction of primary plagioclase. The biotite-plagioclase schists exhibit lower SiO_2 and Al_2O_3, but higher Na_2O and Sr, the latter reflecting the widespread preservation of plagioclase porphyroclasts. Both schist varieties show moderate LREE to HREE fractionation, with relatively flat HREE profiles, moderate Yb_{cn} and Y values, and marked depletion of Ta-Nb, P and Ti compared to adjacent elements on normalized immobile multi-element plots. These features are comparable to those of Phanerozoic calc-alkaline active continental margin sequences. The chlorite schists exhibit somewhat weaker anomalism of Ta-Nb and P, and have a transitional tholeiitic – calc-alkaline signature as indicated by Zr/Y and $[La/Yb]_{cn}$ ratios, but are also similar to modern continental supra-subduction suites. Accordingly, we conclude that the Bien Venue Formation records a period of subduction, volcanism and sedimentation related to a continental arc along the northeastern flank of what is now the BGB, some 30 Ma prior to magmatism in the Kaap Valley - Schoongezicht arc.

The geochemical features of the Bien Venue rocks are distinctly different to patterns recorded for Archaean high-Al TTGs and Cenozoic adakite-bajaite suites derived from anatexis of subducted oceanic slabs. Instead, the observed geochemical data are consistent with an origin via hydrous fusion of mantle-wedge material due to the dehydration of steep subducted oceanic crust.

Despite hosting base-metal mineralization of probable volcanogenic origin, the geochemical characteristics of the Bien Venue rocks are distinctly different to those of most volcanic suites hosting major VHMS ore deposits. Importantly, the rocks appear to have escaped significant fractionation in a high-level magma repository, considered critical in the formation of economic VHMS deposits. These features suggest that the rocks of the Bien Venue Formation in the Three Sisters area are unlikely to host a major VHMS deposit.

ACKNOWLEDGMENTS

The authors wish to thank the Director of the Council for Geoscience, Geological Survey of South Africa for permission to publish this article. We also thank D. Van Graan and L. Von Johnstone for access to properties in the Three Sisters region, and for assistance during fieldwork. Di du Toit drafted the figures and Lucienne Martin provided computer assistance. F.M. Meyer and R.J. Hart assisted with the INAA analyses. The following persons provided insightful discussions on various aspects of the geology of the Bien Venue Formation: M. Cloete, D. R. Lowe, G. R. Byerly, J.H.W. Ward, T.O. Reimer and P. Harrison.

REFERENCES

Abbott, D., Burgess, L., Longhi, J., Smith, W.H.F., 1994. An empirical thermal history of the Earth's upper mantle. J. Geophys. Res., **99**: 13835-13850.

Aggarwal, P.K., Nesbitt, B.E., 1987. Pressure and temperature conditions of metamorphism in the vicinity of three massive sulfide deposits, Flin Flon - Snow Lake belt, Manitoba. Can. J. Earth Sci., **24**: 2305-2315.

Anhaeusser, C.R., 1972. The geology of the Jamestown Hills area of the Barberton Mountain Land, South Africa. Trans. Geol. Soc. S. Afr., **75**: 225-263.

Anhaeusser, C.R., 1973. The evolution of the early Precambrian crust of southern Africa. Phil. Trans. Roy. Soc. Lond., **A273**: 359-388.

Anhaeusser, C.R., 1976. The geology of the Sheba Hills area of the Barberton Mountain Land, South Africa, with particular reference to the Eureka Syncline. Trans. Geol. Soc. S. Afr., **79**: 253-280.

Anhaeusser, C.R., 1980. A geological investigation of the Archaean granite-greenstone terrane south of the Boesmanskop syenite pluton, Barberton Mountain Land. Trans. Geol. Soc. S. Afr., **83**: 93-106.

Anhaeusser, C.R., 1984. Structural elements of Archaean granite-greenstone terranes as exemplified by the Barberton Mountain Land, southern Africa. *In*: Kröner, A. and Greiling, R. (Eds.), *Precambrian Tectonics Illustrated*, E. Schweizerbart'sche Verlagsbuchhandlung, Stuttgart, pp. 57-78.

Anhaeusser, C.R., 1985. Archean layered ultramafic complexes in the Barberton Mountain Land, South Africa. *In*: Ayres, L.D., Thurston, P.C., Card, K.D. and Weber, W. (Eds.), *Evolution of Archean Supracrustal Sequences*, Spec. Pap. Geol. Assoc. Canada **28**: 281-302.

Anhaeusser, C.R., 1986a. The geological setting of chrysotile asbestos occurrences in Southern Africa. *In*: Anhaeusser, C.R. and Maske, S. (Eds.), *Mineral Deposits of Southern Africa*, I, Geol. Soc. S. Afr., pp. 359-375.

Anhaeusser, C.R., 1986b. The Lily gold mine, Barberton greenstone belt: geology, mineralogy and supergene gold enrichment. *In*: Anhaeusser, C.R. and Maske, S. (Eds.), *Mineral Deposits of Southern Africa*, I, Geol. Soc. S. Afr., pp. 187-196.

Anhaeusser, C.R. and Robb, L.J., 1981. Magmatic cycles and the evolution of the Archaean granitic crust in the Eastern Transvaal and Swaziland. Spec. Publ. geol. Soc. Aust., **7**: 457-467.

Anhaeusser, C.R., Robb, L.J. and Viljoen, M.J., 1983. Notes on the provisional geological map of the Barberton greenstone belt and surrounding granitic terrane, Eastern Transvaal and Swaziland (1:250 000 colour map). Spec. Publ. Geol. Soc. S. Afr., **9**: 221-223.

Arculus, R.J., and Powell, R., 1986. Island arc magma sources: a geochemical assessment of the roles of slab-derived components and crustal contamination. Geochem. J., **15**: 109-133.

Arkani-Hamed, J. and Jolly, W.T., 1989. Generation of Archean tonalites. Geology **17**: 307-310.

Armstrong, R.A., Compston, W., De Wit, M.J. and Williams, I.S., 1990. The stratigraphy of the 3.5 - 3.2 Ga Barberton greenstone belt revisited: a single zircon ion microprobe study. Earth Planet. Sci. Lett., **101**: 90-106.

Barley, M.E., 1993. Volcanic, sedimentary and tectonostratigraphic environments of the ~3.46 Ga Warrawoona Megasequence: a review. Precambrian Res., **60**: 47-67.

Barrett, T.J. and MacLean, W.H., 1997. Volcanic sequences, lithogeochemistry and hydrothermal alteration in some bimodal VMS systems. *In*: Barrie, C.T. and Hannington, M.D. (Eds.), *Volcanic –Associated Massive Sulphide Deposits: Processes and Examples in Modern and Ancient Settings*, Geological Association of Canada and The Society of Economic Geologists Co-sponsored Short Course Notes. Carleton University, Ottawa, pp. 105-133.

Barrie, C.T., Ludden, J.N. and Green, T.H., 1993. Geochemistry of volcanic rocks associated with Cu-Zn and Ni-Cu deposits in the Abitibi Subprovince. Econ. Geol., **88**: 1314-1358.

Bohlen, S.R., Montana, A. and Kerrick, D.M., 1991. Precise determinations of the equilibria kyanite± sillimanite and kyanite ± andalusite and a revised triple point for Al_2SiO_5 polymorphs. Amer. Mineralogist **76**: 677-680.

Brenan, J.M., Shaw, H.F., Phinney, D.L. and Ryerson, F.J., 1994. Rutile-aqueous fluid partitioning of Nb, Ta, Hf, Zr, U and Th: implications for high field strength element depletions in island-arc basalts. Earth Planet. Sci. Lett., **128**: 327-339.

Briqueu, L., Bougault, H. and Joron, J.L., 1984. Quantification of Nb, Ta, Ti and V anomalies in magmas associated with subduction zones: petrogenetic implications. Earth Planet. Sci. Lett., **68**: 297-308.

Byerly, G.R., 1999. Komatiites of the Mendon Formation: late-stage ultramafic volcanism in the Barberton greenstone belt. Spec. Pap. Geol. Soc. Amer., **329**: 189-211.

Byerly, G.R., Kröner, A., Lowe, D.R., Todt, W. and Walsh, M.M., 1996. Prolonged magmatism and time constraints for sediment deposition in the Early Archean Barberton greenstone belt: evidence from the Upper Onverwacht and Fig Tree Groups. Precambrian Res.,**78**:125-138.

Calvert, A.J., Sawyer, E.W., Davis, W.J. and Ludden, J.N., 1995. Archaean subduction inferred from seismic images of a mantle suture in the Superior Province. Nature **375**: 670-674.

Car, D. and Ayres, L.D., 1991. A thick dacitic debris flow sequence, Lake of the Woods greenstone terrane, central Canada: resedimented products of Archean vulcanian, plinian and dome-building eruptions. Precambrian Res., **50**: 239 - 260.

Card, K.D., 1990. A review of the Superior Province of the Canadian Shield, a product of Archean accretion. Precambrian Res., **48**: 99-156.

Cas, R.A.F., 1992. Submarine volcanism: eruption styles, products, and relevance to understanding the host-rock successions to volcanic-hosted massive sulfide deposits. Econ. Geol., **87**: 511 - 541.

Cas, R.A.F. and Wright, J.V., 1987. *Volcanic Successions - Modern and Ancient. A Geological Approach to Processes, Products and Successions.* Allen and Unwin, London.

Cassidy, K.F., Barley, M.E., Groves, D.I., Perring, C.S. and Hallberg, J.A., 1991. An overview of the nature, distribution and inferred tectonic setting of granitoids in the late-Archaean Norseman-Wiluna belt. Precambrian Res., **51**: 51-83.

Chatterjee, N.D. and Johannes, W., 1974. Thermal stability and standard thermodynamic properties of synthetic 2M1-muscovite, $KAl_2[AlSi_3O_{10}(OH)_2]$. Contr. Mineral. Petrol., **48**: 89-114.

Cloete, M., 1999. Aspects of volcanism and metamorphism of the Onverwacht Group lavas in the southwestern portion of the Barberton greenstone belt. Mem. Geol. Surv. S. Afr., **84**, 232pp.

Condie, K.C., 1986. Geochemistry and tectonic setting of early Proterozoic supracrustal rocks in the southwestern United States. J. Geol., **94**: 845-864.

Condie, K.C., 1989. Geochemical changes in basalts and andesites across the Archean-Proterozoic boundary: identification and significance. Lithos **23**: 1-18.

Condie, K.C., Macke, J.E. and Reimer, T.O., 1970. Petrology and geochemistry of early Precambrian graywackes from the Fig Tree Group, South Africa. Bull. Geol. Soc. Amer., **81**: 2759-2776.

Cullers, R.L., DiMarco, M.J., Lowe, D.R. and Stone, J., 1993. Geochemistry of a silicified, felsic volcaniclastic suite from the early Archaean Panorama Formation, Pilbara Block, Western Australia: an evaluation of depositional and post-depositional processes with special emphasis on the rare-earth elements. Precambrian Res., **60**: 99-116.

Defant, M.J. and Drummond, M.S., 1990. Derivation of some modern arc magmas by melting of young subducted lithosphere. Nature **347**: 662-665.

de Ronde, C.E.J. and de Wit, M.J., 1994. The tectonic history of the Barberton greenstone belt, South Africa: ~490 million years of Archean crustal evolution. Tectonics **13**: 983-1005.

de Wit, M.J., 1982. Gliding and overthrust nappe tectonics in the Barberton greenstone belt. J. Struct. Geol., **4**: 117-136.

de Wit, M.J., 1983. Notes on a preliminary 1:25 000 geological map of the southern part of the Barberton greenstone belt. Spec. Publ. Geol. Soc. S. Afr., **9**: 185-187.

de Wit, M.J., Fripp, R.E.P., Stanistreet, I.G., 1983. Tectonic and stratigraphic implications of new field observations along the southern part of the Barberton greenstone belt. Spec. Publ. Geol. Soc. S. Afr., **9**: 21-29.

de Wit, M.J., Armstrong, R., Hart, R.J. and Wilson, A.H., 1987a. Felsic igneous rocks within the 3.3- to 3.5-Ga Barberton greenstone belt: high crustal level equivalents of the surrounding tonalite-trondhjemite terrain, emplaced during thrusting. Tectonics **6**: 529-549.

de Wit, M.J., Hart, R.A. and Hart, R.J., 1987b. The Jamestown Ophiolite Complex, Barberton mountain belt: a section through 3.5 Ga oceanic crust. J. Afr. Earth Sci., **6**: 681-730.

de Wit, M.J., Roering, C., Hart, R.J., Armstrong, R.A., de Ronde, C.E.J., Green, R.W.E., Tredoux, M., Peberdy, E. and Hart, R.A., 1992. Formation of an Archaean continent. Nature **357**: 553-562.

Drummond, M.S., Defant, M.J. and Kepezhinskas, P.K., 1996. Petrogenesis of slab-derived trondhjemite-tonalite-dacite/adakite magmas. Trans. Roy. Soc. Edinburgh: Earth Sci., **87**: 205-215.

Dolozi, M.D. and Ayres, L.D., 1991. Early Proterozoic basaltic andesite tuff-breccia: downslope, subaqueous mass transport of phreatomagmatically-generated tephra. Bull. Volcanol., **53**: 477-495.

Dostal, J., Keppie, J.D. and Zhai, M., 1992. Geochemistry of mineralized and barren, Late Proterozoic felsic volcanic rocks in southeastern Cape Breton Island, Nova Scotia (Canada). Precambrian Res., **56**: 33-49.

Dupré, B. and Arndt, N.T., 1990. Pb isotopic compositions of Archean komatiites and sulfides. Chem. Geol., **85**: 35-56.

Erasmus, C. S., Fesq, H.W., Kable, E.J.D., Rasmussen, S.E. and Sellschop, J.P.F., 1977. The NIMROC samples as reference materials for neutron activation analysis. J. Radioanal. Chem., **39**: 323-334.

Eriksson, K.A., 1980a. Hydrodynamic and paleogeographic interpretation of turbidite deposits from the Archean Fig Tree Group of the Barberton Mountain Land, South Africa. Bull. Geol. Soc. Amer., **91**: 21-26.

Eriksson, K.A., 1980b. Transitional sedimentation styles in the Moodies and Fig Tree Groups, Barberton Mountain Land, South Africa: evidence favouring an Archean continental margin. Precambrian Res., **12**: 141-160.

Ewart, A., 1982. The mineralogy and petrology of Tertiary - Recent orogenic rocks: with special reference to the andesitic - basaltic compositional range. *In*: Thorpe, R.S. (Ed.), *Andesites: Orogenic Andesites and Related Rocks*. John Wiley and Sons, Chichester, pp. 25-95.

Feng, R. and Kerrich, R., 1992. Geochemical evolution of granitoids from the Archean Abitibi Southern Volcanic Zone and Pontiac subprovince, Superior Province, Canada: implications for tectonic history and source regions. Chem. Geol., **98**: 23-70.

Feng, R., Jianzhong, F. and Kerrich, R., 1993. Noble metal abundances and characteristics of six granitic magma series, Archean Abitibi Belt, Pontiac Subprovince: relationships to metallogeny and overprinting of mesothermal gold deposits. Econ. Geol., **88**: 1376-1401.

Fesq, H.W., Bibby, D.M., Sellschop, J.P.F. and Watterson, J.I.W., 1973. The determination of trace element impurities in natural diamonds by instrumental neutron activation analysis. J. Radioanal. Chem.,**17**: 195-216.

Finlow-Bates, T. and Stumpfl, E.F., 1981. The behaviour of so-called immobile elements in hydrothermally altered rocks associated with volcanogenic submarine-exhalative ore deposits. Mineral. Deposita **16**: 319-328.

Fouquet, Y., Von Stackelberg, U., Charlou, J.L., Erzinger, J., Mühe, R. and Wiedicke, M., 1993. Metallogenesis in back-arc environments: the Lau Basin example. Econ. Geol., **88**: 2154-2181.

Frater, K.M., 1983. Effects of metasomatism and development of quartz 'eyes' in intrusive and extrusive rocks at Golden Grove Cu-Zn deposit, Western Australia. Trans. Instn. Min. Metall. **B92**: 121-131.

Fryer, P., Taylor, B., Langmuir, C.H. and Hochstaedter, A.G., 1990. Petrology and geochemistry of lavas from the Sumisu and Torishima backarc rifts. Earth Planet. Sci. Lett., **100**: 161-178.

Ganguly, J., 1969. Chloritoid stability and related parageneses: theory, experiments, and applications. Amer. J. Sci., **267**: 910-944.

Glikson, A.Y., 1976. Trace element geochemistry and origin of early Precambrian acid igneous series, Barberton Mountain Land, Transvaal. Geochim. Cosmochim. Acta **40**: 1261-1280.

Goldstein, A., Pickens, J., Klepeis, K. and Linn, F., 1995. Finite strain heterogeneity and volume loss in slates of the Taconic Allochthon, Vermont, U.S.A. J. Struct. Geol., **17**: 1207-1216.

Guber, A.L. and Merrill, S., 1983. Paleobathymetric significance of the formaminifera from the Hokuroku District. Econ. Geol. Mon., **5**: 55-70.

Hall, A.L., 1918. The geology of the Barberton gold mining district. Mem. Geol. Surv. S. Afr., **9**, 347 pp.

Harris, N.B.W., Pearce, J.A. and Tindle, A.G., 1986. Geochemical characteristics of collision-zone magmatism. *In*: Coward, M.P. and Ries, A.C. (Eds.), *Collision Tectonics*. Spec. Publ. Geol. Soc., **19**: 67-81.

Harwood, A. and Murphy, P.W., 1988. The petrology of the Bien Venue polymetallic massive sulphide deposit, Eastern Transvaal. Ext. Abstr. Geocongress '88, Univ. Natal, Durban, 811-812.

Hawkesworth, C.J., Gallagher, K., Hergt, J.M. and McDermott, F., 1993. Mantle and slab contribution in arc magmas. Ann. Rev. Earth Planet. Sci., **21**: 175-204.

Heinrichs, T.K. and Reimer, T.O., 1977. A sedimentary barite deposit from the Archean Fig Tree Group of the Barberton Mountain Land (South Africa). Econ. Geol., **72**: 1426-1441.

Hemley, J.J., Montoya, J.W., Marinenko, J.W. and Luce, R.W., 1980. Equilibria in the system Al_2O_3-SiO_2-H_2O and some general implications for alteration / mineralization processes. Econ. Geol., **75**: 210-228.

Heubeck, C. and Lowe, D.R., 1994a. Depositional and tectonic setting of the Archean Moodies Group, Barberton greenstone belt, South Africa. Precambrian Res., **68**: 257-290.

Heubeck, C. and Lowe, D.R., 1994b. Late syndepositional deformation and detachment tectonics in the Barberton greenstone belt, South Africa. Tectonics **13**: 1514 -1536.

Heubeck, C. and Lowe, D.R., 1999. Sedimentary petrography and provenance of the Archean Moodies Group, Barberton greenstone belt. Spec. Pap. Geol. Soc. Amer., **329**: 259-286.

Heubeck, C., Wendt, J.I., Toulkeridis, T., Kröner, A. and Lowe, D.R., 1993. Timing of deformation of the early Archaean Barberton greenstone belt, South Africa: constraints from zircon dating of the Salisbury Kop pluton. Trans. Geol. Soc. S. Afr., *96*: 1-8.

Hildreth, W. and Moorbath, S., 1988. Crustal contributions to arc magmatism in the Andes of Central Chile. Contr. Mineral. Petrol., **98**: 455-489.

Jackson, M.P.A. and Robertson, D.I., 1983. Regional implications of early-Precambrian strains in the Onverwacht Group adjacent to the Lochiel Granite, north-west Swaziland. Spec. Publ. Geol. Soc. S. Afr., 9: 45-62.

Jackson, M.P.A., Eriksson, K.A. and Harris, C.W., 1987. Early Archean foredeep sedimentation related to crustal shortening: a reinterpretation of the Barberton Sequence, southern Africa. Tectonophysics **136**: 197-221.

Jackson, S. L. and Cruden, A.R., 1995. Formation of the Abitibi greenstone belt by arc-trench migration. Geology **23**: 471-474.

Jackson, S.L., Fyon, J. A. and Corfu, F., 1994. Review of Archean supracrustal assemblages of the southern Abitibi greenstone belt in Ontario, Canada: products of microplate interaction within a large-scale plate-tectonic setting. Precambrian Res., **65**: 183-205.

Kamo, S. L. and Davis, D.W., 1994. Reassessment of Archean crustal development in the Barberton Mountain Land, South Africa, based on U-Pb dating. Tectonics **13**: 167-192.

Kelemen, P.B., Shimizu, N. and Dunn, T., 1993. Relative depletion of niobium in some arc magmas and the continental crust: partitioning of K, Nb, La and Ce during melt / rock reaction in the upper mantle. Earth. Planet. Sci. Lett., **120**: 111-134.

Kimura, M., Uyeda, S., Kato, Y., Tanaka, T., Yamano, M., Gamo, T., Sakai, H., Kato, S., Izawa, E. and Oomori, T., 1988. Active hydrothermal mounds in the Okinawa Trough back-arc basin, Japan. Tectonophysics **145**: 319-324.

Kisters, A.F.M. and Anhaeusser, C.R., 1995a. Emplacement features of Archaean TTG plutons along the southern margin of the Barberton greenstone belt, South Africa. Precambrian Res., **75**: 1-15.

Kisters, A.F.M. and Anhaeusser, C.R., 1995b. The structural significance of the Steynsdorp pluton and anticline within the tectono-magmatic framework of the Barberton Mountain Land.
S. Afr. J. Geol., **98**: 43-51.

Kohler, E.A., 1994. *The geology of the Archaean granitoid-greenstone terrane in the vicinity of Three Sisters, Barberton greenstone belt.* Ph.D. thesis (unpubl.), Univ. Witwatersrand, Johannesburg, 309pp.

Kohler, E. A., 2000. The geology of the Archaean granitoid-greenstone terrane in the vicinity of Three Sisters, Barberton greenstone belt. Bulletin of the Council for Geoscience, Geol. Surv. S. Afr., (in press).

Kröner, A. and Todt, W., 1988. Single zircon dating constraining the maximum age of the Barberton greenstone belt, southern Africa. J. Geophys. Res., **93**: 15329-15337.

Kröner, A., Byerly, G.R. and Lowe, D.R., 1991. Chronology of early Archaean granite-greenstone evolution in the Barberton Mountain Land, South Africa, based on precise dating by single zircon evaporation. Earth Planet. Sci. Lett., **103**: 41-54.

Kröner, A., Hegner, E., Wendt, J.I. and Byerly, G.R., 1996. The oldest part of the Barberton granitoid-greenstone terrain, South Africa: evidence for crust formation between 3.5 and 3.7 Ga. Precambrian Res., **78**: 105-124.

Lahaye, Y., Arndt, N., Byerly, G., Chauvel, C., Fourcade, S. and Gruau, G., 1995. The influence of alteration on the trace-element and Nd isotopic compositions of komatiites. Chem. Geol., **126**: 43-64.

Lamb, S.H., 1984. Structures on the eastern margin of the Archaean Barberton greenstone belt, northwest Swaziland. *In*: Kröner, A. and Greiling, R. (Eds.), *Precambrian Tectonics Illustrated*. E. Schweizerbart'sche Verlagsbuchhandlung, Stuttgart, pp. 19-39.

Lamb, S., 1987. Archean synsedimentary tectonic deformation - a comparison with the Quaternary. Geology **15**: 565-568.

Lamb, S. and Paris, I., 1988. Post-Onverwacht Group stratigraphy in the SE part of the Archaean Barberton greenstone belt. J. Afr. Earth Sci., **7**: 285-306.

Lanier, W. P. and Lowe, D.R., 1982. Sedimentology of the Middle Marker (3.4 Ga), Onverwacht Group, Transvaal, South Africa. Precambrian Res., **18**: 237-260.

Larson, J.E. and Hutchinson, R.W., 1993. The Selbaie Zn-Cu-Ag deposits, Quebec, Canada: an example of evolution from subaqueous to subaerial volcanism and mineralization in an Archean caldera environment. Econ. Geol., **88**: 1460-1482.

Layer, P.W., Kröner, A., McWilliams, M. and York, D., 1989. Elements of the Archean thermal history and apparent polar wander of the eastern Kaapvaal Craton, Swaziland, from single grain dating and paleomagnetism. Earth Planet. Sci. Lett., **93**: 23-34.

Layer, P.W., Lopez-Martinez, M., Kröner, A., York, D. and McWilliams, M., 1998. Thermochronometry and palaeomagnetism of the Archaean Nelshoogte pluton, South Africa. Geophys. J. Int., **135**: 129-145.

Lesher, C.M., Goodwin, A.M., Campbell, I.H. and Gorton, M.P., 1986. Trace-element geochemistry of ore-associated and barren, felsic metavolcanic rocks in the Superior Province, Canada. Can. J. Earth Sci., **23**: 222-237.

Lizasa, K., Fiske, R.S., Ishizuka, O., Yuasa, M., Hashimoto, J., Ishibashi, J., Naka, J., Horii, Y., Fijuwara, Y., Imai, A. and Koyama, S., 1999. A Kuroko-type polymetallic sulfide deposit in a submarine silicic caldera. Science **283**: 975-977.

Lowe, D.R, 1999. Geologic evolution of the Barberton greenstone belt and vicinity. Spec. Pap. Geol. Soc. Amer., **329**: 287-312.

Lowe, D.R. and Knauth, L.P., 1977. Sedimentology of the Onverwacht Group (3.4 billion years), Transvaal, South Africa, and its bearing on the characteristics and evolution of the early Earth.
J. Geol., **85**: 699-723.

Lowe, D.R. and Byerly, G.R., 1999. Stratigraphy of the west-central part of the Barberton greenstone belt, South Africa. Spec. Pap. Geol. Soc. Amer., **329**: 1-36.

Lowe, D. R. and Nocita, B.W., 1999. Foreland basin sedimentation in the Mapepe Formation, southern-facies Fig Tree Group. Spec. Pap. Geol. Soc. Amer., **329**: 233-258.

Lowe, D.R., Byerly, G.R., Ransom, B.L., and Nocita, B.W., 1985. Stratigraphic and sedimentological evidence bearing on structural repetition in early Archaean rocks of the Barberton greenstone belt, South Africa. Precambrian Res., **27**: 165-186.

Lowe, D.R., Byerly, G.R. and Heubeck, C., 1999. Structural divisions and development of the west-central part of the Barberton greenstone belt. Spec. Pap. Geol. Soc. Amer., **329**: 37-82.

MacLean, W.H., 1990. Mass change calculations in altered rock series. Mineral Deposita **25**:44 -49.

MacLean, W.H. and Barrett, T.J., 1993. Lithogeochemical techniques using immobile elements.
J. Geochem. Exp., **48**: 109-133.

MacLean, W.H. and Kranidiotis, P., 1987. Immobile elements as monitors of mass transfer in hydrothermal alteration: Phelps Dodge massive sulfide deposit, Matagami, Quebec. Econ. Geol., **82**: 951-962.

Maphalala, R.M. and Kröner, A., 1993. Pb-Pb single zircon ages for the younger Archaean granitoids of Swaziland, southern Africa. Ext. Abstr. 16th Int. Coll. Afr. Geol., Mbabane, pp. 201-206.

Martin, H., 1986. Effect of steeper Archaean geothermal gradient on geochemistry of subduction-related magmas. Geology **14**: 753-756.

Martin, H., 1993. The mechanisms of petrogenesis of the Archaean continental crust - comparison with modern processes. Lithos **30**: 373-388.

McCulloch, M.T., 1993. The role of subducted slabs in an evolving earth. Earth Planet. Sci. Lett., **115**: 89-100.

Murphy, P.W., 1990. *The petrology, geochemistry and classification of the Bien Venue massive sulphide deposit, Barberton Mountain Land.* M.Sc. thesis (unpubl.), Univ. Natal, Durban, 111pp.

Norrish, K. and Hutton, T.J., 1969. An accurate X-ray spectrograph method for the analysis of a wide range of geological samples. Geochim. Cosmochim. Acta **33**: 431-453.

Nocita, B.W. and Lowe, D.R., 1990. Fan-delta sequence in the Archean Fig Tree Group, Barberton greenstone belt, South Africa. Precambrian Res., **48**: 375-393.

Paris, I.A., 1990. Depositional environment of the Onverwacht sedimentary rocks, Barberton greenstone belt, South Africa. J. Afr. Earth Sci., **10**: 509-518.

Paris, I.A., Stanistreet, I.G. and Hughes, M.J., 1985. Cherts of the Barberton greenstone belt interpreted as products of submarine exhalative activity. J. Geol., **93**: 111-129.

Pattison, D.M.R., 1992. Stability of andalusite and sillimanite and the Al_2SiO_5 triple point: constraints from the Ballachulish aureole, Scotland. J. Geol., **100**: 423-446.

Pearce, J.A., 1982. Trace element characteristics of lavas from destructive plate boundaries. *In*: Thorpe, R.S. (Ed.), *Andesites: Orogenic Andesites and Related Rocks.* John Wiley and Sons, Chichester, pp. 525-548.

Pearce, J.A., 1983. Role of the sub-continental lithosphere in magma genesis at active continental margins. *In*: Hawkesworth, C.J. and Norry, M.J. (Eds.), *Continental Basalts and Mantle Xenoliths.* Shiva, Nantwich, pp. 230-249.

Pearce, J. A. and Peate, D.W., 1995. Tectonic implications of the composition of volcanic arc magmas. Ann. Rev. Earth Planet. Sci., **23**: 251-285.

Pearce, J.A., Harris, N.B.W. and Tindle, A.G., 1984. Trace element discrimination diagrams for the tectonic interpretation of granitic rocks. J. Petrol., **25**: 956-983.

Pisutha-Arnond, V. and Ohmoto, H., 1983. Thermal history, and chemical and isotopic compositions of the ore-forming fluids responsible for the Kuroko massive sulfide deposits in the Hokuroku District of Japan. Econ. Geol. Mon., **5**: 523-558.

Reimer, T.O., 1980. Archean sedimentary baryte deposits of the Swaziland Supergroup (Barberton Mountain Land, South Africa). Precambrian Res., **12**: 393-410.

Ricketts, B.D., Ware, M.J. and Donaldson, J.A., 1982. Volcaniclastic rocks and volcaniclastic facies in the middle Precambrian (Aphebian) Belcher Group, Northwest Territories, Canada. Can. J. Earth Sci., **19**: 1275-1294.

Robb, L.J., Anhaeusser, C.R. and Van Nierop, D.A., 1983. The recognition of the Nelspruit batholith north of the Barberton greenstone belt and its significance in terms of Archaean crustal evolution. Spec. Publ. Geol. Soc. S. Afr., **9**: 117-130.

SACS (South African Committee for Stratigraphy), 1980. Stratigraphy of South Africa: Part 1 - Lithostratigraphy of the Republic of South Africa, South West Africa / Namibia and the Republics of Bophuthatswana, Transkei and Venda. Handbk. Geol. Surv. S. Afr., **8**, 690pp.

Saunders, A.D., Tarney, J. and Weaver, S.D., 1980. Transverse geochemical variations across the Antarctic Peninsula: implications for the genesis of calc-alkaline magmas. Earth Planet. Sci. Lett., **46**: 344-360.

Saunders, A.D., Roger, G., Marriner, G.F., Terrell, D.J. and Verma, S.P., 1987. Geochemistry of Cenozoic volcanic rocks, Baja California, Mexico: implications for the petrogenesis of post-subduction magmas. J. Volcanol. Geotherm. Res., **32**: 223-245.

Shervais, J.W., 1982. Ti-V plots and the petrogenesis of modern and ophiolitic lavas. Earth Planet. Sci. Lett., **59**: 101-118.

Sleep, N.H. and Windley, B.F., 1982. Archean plate tectonics: constraints and inferences.
J. Geol., **90**: 363-379.

Stolz, A.J., Varne, R., Davies, G.R., Wheller, G. E. and Foden, J.D., 1990. Magma source components in an arc - continent collision zone: the Flores - Lembata sector, Sunda arc, Indonesia. Contr. Mineral. Petrol., **105**: 585-601.

Sun, S. and McDonough, W.F., 1989. Chemical and isotopic systematics of ocean basalts: implications for mantle composition and processes. *In*: Saunders, A.D. and Norry, M.J. (Eds.), *Magmatism in the Ocean Basins*, Geol. Soc. Spec. Publ., **42**, Blackwell Scientific, Oxford, pp. 313-345.

Sutcliffe, R.H., Barrie, C.T., Burrows, D. R. and Beakhouse, G.P., 1993. Plutonism in the southern Abitibi Subprovince: a tectonic and petrogenetic framework. Econ. Geol., **88**: 1359-1375.

Tan, B.T., Gray, D. R. and Stewart, I., 1995. Volume change accompanying cleavage development in graptolitic shales from Gisborne, Victoria, Australia. J. Struct. Geol., **17**: 1387-1394.

Tarney, J. and Jones, C. E., 1994. Trace element geochemistry of orogenic igneous rocks and crustal growth models. J. Geol. Soc., **151**: 855-868.

Tegtmeyer, A.R. and Kröner, A., 1987. U-Pb zircon ages bearing on the nature of early Archaean
greenstone belt evolution, Barberton Mountain Land, southern Africa. Precambrian Res., **36**: 1-20.

Tomkinson, M.J., and Lombard, A., 1990. Structure, metamorphism and mineralization in the New Consort Gold Mines, Barberton greenstone belt, South Africa. Ext. Abstr. 3rd Int. Archaean Symposium, Perth, pp.377-379.

Urabe, T. and Kusakabe, M., 1990. Barite silica chimneys from the Sumisu Rift, Izu-Bonin Arc: possible analog to hematitic chert associated with Kuroko deposits. Earth Planet. Sci. Lett., **100**: 283-290.

Van Bergen, M.J., Vroon, P.Z., Varekamp, J.C. and Poorter, R.P.E., 1992. The origin of the potassic rock suite from Batu Tara volcano (East Sunda arc, Indonesia). Lithos **28**: 261-282.

Vance, R.K. and Condie, K.C., 1987. Geochemistry of footwall alteration associated with the Early Proterozoic United Verde massive sulphide deposit, Jerome, Arizona. Econ. Geol., **82**: 571-586.

Vearncombe, S. and Kerrich, R., 1999. Geochemistry and geodynamic setting of volcanic and plutonic rocks associated with Early Archaean volcanogenic massive sulphide mineralization, Pilbara Craton. Precambrian Res., **98**: 243-270.

Vernon, R.H., 1986. Evaluation of the "quartz-eye" hypothesis. Econ. Geol., **81**: 1520-1527.

Viljoen, M.J. and Viljoen, R.P., 1969a. An introduction to the geology of the Barberton granite-greenstone terrain. Spec. Publ. Geol. Soc. S. Afr., **2**: 9-28.

Viljoen, M.J. and Viljoen, R.P., 1969b. The geology and geochemistry of the lower ultramafic unit of the Onverwacht Group and a proposed new class of igneous rocks. Spec. Publ. Geol. Soc. S. Afr., **2**: 55-85.

Viljoen, R. P. and Viljoen, M.J., 1969a. The geological and geochemical significance of the upper formations of the Onverwacht Group. Spec. Publ. Geol. Soc. S. Afr., **2**: 113-151.

Viljoen, R. P. and Viljoen, M.J., 1969b. The relationship between mafic and ultramafic magma derived from the upper mantle and the ore deposits of the Barberton region. Spec. Publ. Geol. Soc. S. Afr., **2**: 221-244.

Viljoen, R.P. and Viljoen, M.J., 1970. The geology and geochemistry of the layered bodies of the Kaapmuiden area, Barberton Mountain Land. Spec. Publ. Geol. Soc. S. Afr., **1**: 661-688.

Viljoen, R.P., Saager, R. and Viljoen M.J., 1969. Metallogenesis and ore control in the Steynsdorp Goldfield, Barberton Mountain Land. Econ. Geol., **64**: 778-797.

Visser, D.J.L. (Compiler), 1956. The geology of the Barberton area. Spec. Publ. Geol. Surv. S. Afr., **15**, 242pp.

Whitford, D.J., McPherson, W.P.A. and Wallace, D.B., 1989. Geochemistry of the host rocks of the volcanogenic massive sulfide deposit at Que River, Tasmania. Econ. Geol., **84**: 1-21.

Williams, D.A.C. and Furnell, R.G., 1979. Reassessment of part of the Barberton type area, South Africa. Precambrian Res., **9**: 325-347.

Williams, M. L. and Burr, J.L., 1994. Preservation and evolution of quartz phenocrysts in deformed rhyolites from the Proterozoic of southwestern North America. J. Struct. Geol., **16**: 203-221.

Winchester, J.A. and Floyd, P.A., 1977. Geochemical discrimination of different magma series and their differentiation products using immobile elements. Chem. Geol., **20**: 325-343.

Windley, B.F., 1993. Uniformitarianism today: plate tectonics is the key to the past. J. Geol. Soc. Lond., **150**: 7-19.

Wright, I.C., De Ronde, C.E.J., Faure, K. and Gamble, J.A., 1998. Discovery of hydrothermal sulfide mineralization from southern Kermadec arc volcanoes (SW Pacific). Earth Planet. Sci. Lett., **163**: 335-243.

Zhou, T., Dong, G. and Phillips, G.N., 1994. Chemographic analysis of assemblages involving pyrophyllite, chloritoid, chlorite, kaolinite, kyanite, quartz: application to metapelites in the Witwatersrand goldfields, South Africa. J. Metam. Geol., **12**: 655-666.

oOo

APPENDIX

Table 1. Major (wt%) and trace element (ppm) analyses of quartz-muscovite schists, Bien Venue Formation (b = below detection limit)

Sample	BVR1	BVR2	BVR3	BVR4	BVR5	BVR6	BVR7	BVR8	BVR9	BVR10	BVR11	BVR12	BVR13	BVR14	BVR15	BVR16	BVR17	BVR18
SiO_2	74.55	76.57	78.76	71.73	72.04	72.47	74.28	73.90	75.16	78.26	72.57	73.51	72.01	69.25	66.88	63.36	73.06	79.71
TiO_2	0.58	0.36	0.36	0.58	0.47	0.59	0.47	0.51	0.56	0.60	0.48	0.45	0.56	0.65	0.61	0.25	0.50	0.52
Al_2O_3	16.21	15.39	12.86	18.37	16.87	18.64	17.29	18.01	16.11	16.05	17.15	17.04	16.62	18.56	19.46	16.48	18.95	13.53
$Fe_2O_3^{total}$	0.23	3.44	0.75	2.92	3.93	2.68	1.90	2.68	3.02	0.87	4.08	2.81	3.35	3.38	2.03	2.92	1.60	0.93
MnO	b	0.14	0.02	0.06	0.27	0.18	0.11	0.25	0.15	b	0.32	0.17	0.20	0.14	0.01	0.10	0.13	0.02
MgO	0.37	0.58	3.85	0.45	0.52	0.31	0.18	0.24	0.37	0.11	0.41	0.38	0.88	0.61	2.17	2.24	0.26	0.34
CaO	0.33	0.14	0.02	0.30	0.08	0.03	0.01	0.08	0.27	0.25	0.12	0.08	0.30	0.12	1.15	3.62	0.07	0.09
Na_2O	b	0.26	b	0.19	b	0.26	b	0.25	b	0.25	b	0.27	0.32	0.35	3.77	0.43	0.31	b
K_2O	3.81	2.71	2.22	4.01	1.96	1.62	2.10	1.36	2.07	2.03	1.72	2.32	3.30	3.96	1.64	6.24	2.35	2.14
P_2O_5	0.15	0.12	0.02	0.16	0.06	0.51	0.04	0.09	0.16	0.16	0.11	0.11	0.17	0.17	0.28	0.08	0.10	0.10
LOI	1.98	1.86	2.23	1.96	2.34	2.85	2.63	2.80	2.21	1.50	2.55	2.59	2.25	2.52	2.42	4.35	3.02	1.82
Total	98.21	101.57	101.09	100.73	98.54	100.14	99.01	100.17	100.08	100.08	99.51	99.73	99.96	99.71	100.42	100.07	100.35	99.20
Ba	299	116	220	103	198	104	120	138	96	98	121	115	176	220	183	236	121	139
Rb	77	65	61	49	124	47	52	35	66	50	42	57	74	91	58	111	50	48
Sr	33	9	26	12	38	39	19	21	18	12	19	28	26	42	120	33	29	17
Cs		4.67		2.32		4.13		3.63		2.92		4.16	5.51	6.70	1.86	6.05	4.24	
Pb	6	5	6	6	8	9	8	9	8	7	8	9	5	6	12	15	7	5
U		1.61		0.72		0.84		1.47		1.07		1.77	1.03	1.23	1.16	1.66	1.87	
Th		5.35		3.52		4.27		4.70		2.84		5.81	3.36	4.13	4.51	6.92	5.98	
Y	21	21	21	23	26	23	22	25	19	19	20	26	21	23	39	19	24	25
Nb	9	9	6	14	13	14	15	13	13	12	14	15	10	12	19	12	15	15
Zr	131	85	169	141	147	152	147	145	140	142	138	145	148	171	241	96	160	232
Hf		3.51		2.71		3.76		3.74		3.27		3.62	3.76	4.43	5.34	2.83	4.30	
Ta		1.02		0.75		0.85		0.94		0.64		1.10	0.73	0.82	1.14	1.13	1.13	
Ga	22	21	20	22	23	22	22	21	19	20	22	22	21	23	25	18	23	19
V	79	57	29	74	90	74	60	72	59	74	65	64	111	125	116	49	86	53
Cr	50	14	5	20	37	37	21	37	43	56	25	23	73	82	34	78	49	27
Sc		8.18		6.58		10.40		8.37		6.57		6.65	9.87	11.20	12.90	4.51	6.09	
Zn	18	23	44	18	18	17	13	17	15	11	23	19	21	19	66	38	19	12
Cu	18	15	13	9	9	14	12	8	10	10	18	20	10	17	14	22	16	13
Ni	20	24	12	23	28	56	17	13	28	22	27	23	33	22	11	18	15	12
Co		10.40		3.32		8.95		1.40		1.78		3.74	7.77	4.09	6.28	7.32	1.73	
La		24.5		16.3		21.7		24.6		19.6		26.5	23.5	25.8	33.6	26.1	31.6	
Ce		50.5		32.5		46.6		50.1		42.0		55.0	51.7	55.9	76.7	55.3	61.4	
Nd		22.2		15.9		21.4		21.3		20.7		22.5	20.7	25.7	33.9	20.1	27.4	
Sm		3.76		2.48		3.35		3.68		3.28		3.78	3.79	4.20	6.19	3.27	4.47	
Eu		1.06		0.74		0.95		1.14		0.90		0.99	1.15	1.31	1.83	0.72	1.12	
Tb		0.59		0.47		0.60		0.60		0.53		0.60	0.59	0.65	0.96	0.52	0.62	
Yb		2.35		1.61		2.22		2.51		1.20		2.51	2.49	2.49	3.51	2.32	2.46	
Lu		0.25		0.22		0.31		0.41		0.22		0.31	0.32	0.51	0.45	0.33	0.32	
K_2O/Na_2O		10.4		21.1		6.2		5.4		8.1		8.6	10.3	11.3	0.44	14.5	7.6	
K_2O/CaO	19.4	111.0	13.4	24.5	54.0	210.0	17.0	7.7	8.1	14.3	29.0	11.0	33.0	1.4	1.7	33.6	23.8	4.2
Sr/Y	1.57	0.43	1.24	0.52	1.46	1.70	0.86	0.84	0.95	0.63	0.95	1.08	1.24	1.83	3.08	1.74	1.21	0.68
Zr/Y	6.2	4.0	8.0	6.1	5.7	6.6	6.7	5.8	7.4	7.5	6.9	5.6	7.0	7.4	6.2	5.1	6.7	9.3
Nb/Y	0.43	0.43	0.29	0.61	0.50	0.61	0.68	0.52	0.68	0.63	0.70	0.58	0.48	0.52	0.49	0.63	0.63	0.60
Ti/Zr	26.5	25.4	12.8	24.6	19.2	23.3	19.2	21.1	24.0	25.3	20.8	18.6	22.7	22.8	15.2	15.6	18.7	13.4
Th/Yb		2.3		2.2		1.9		1.9		2.4		2.3	1.3	1.7	1.3	3.0	2.4	
[La/Yb]cn		7.5		7.3		7.0		7.0		11.7		7.6	6.8	7.4	6.9	8.1	9.2	
[Tb/Yb]cn		1.14		1.33		1.23		1.09		2.01		1.09	1.08	1.19	1.24	1.02	1.15	
Eu/Eu*		0.93		0.89		0.87		1.00		0.89		0.86	1.00	1.03	0.98	0.72	0.88	

Table 2. Major (wt%) and trace element (ppm) analyses of biotite – oligoclase schists, Bien Venue Formation (b = below detection limit)

Sample	BVD1	BVD2	BVD3	BVD4	BVD5	BVD6	BVD7
SiO_2	67.23	68.83	67.75	69.63	70.33	69.77	65.67
TiO_2	0.44	0.41	0.43	0.50	0.52	0.50	0.62
Al_2O_3	15.42	13.08	15.38	12.94	13.53	12.94	14.85
$Fe_2O_3^{total}$	3.97	4.00	4.32	2.95	3.55	3.75	4.49
MnO	0.05	0.07	0.04	0.07	0.06	0.07	0.06
MgO	3.33	2.81	4.33	1.49	2.48	2.34	4.13
CaO	1.01	2.53	0.99	2.71	1.86	2.81	0.88
Na_2O	5.42	3.70	4.20	5.19	3.64	4.56	4.42
K_2O	2.54	1.50	0.89	2.11	3.32	2.07	3.17
P_2O_5	0.14	0.16	0.13	0.12	0.12	0.11	0.15
H_2O-	0.01	0.02	0.02	0.12	0.02	0.03	0.05
H_2O+	0.46	0.58	1.70	0.38	0.26	0.34	0.56
CO_2	0.08	0.88	0.13	1.43	0.11	1.04	0.08
Total	100.10	98.57	100.31	99.64	99.80	100.33	99.13
Ba	213	157	83	367	495	97	195
Rb	69	66	38	41	100	57	75
Sr	73	77	90	129	85	99	66
Cs	7.59	5.48			4.53	2.09	7.27
Pb	12	9	5	b	13	b	7
U	1.22	1.03			1.19	0.82	1.07
Th	3.96	3.49			4.78	4.63	4.09
Y	14	18	15	17	18	14	17
Nb	7	8	7	11	10	10	11
Zr	86	105	79	115	121	111	126
Hf	3.20	3.52			3.42	3.18	3.39
Ta	0.80	0.76			0.90	0.89	0.85
Ga	22	19	22	13	13	12	16
V	68	55	70	53	55	50	77
Cr	47	44	37	7	8	7	42
Sc	8.28	7.53			6.61	6.34	9.33
Zn	51	57	26	40	100	45	53
Cu	28	21	14	42	43	11	10
Ni	47	40	45	22	22	26	45
Co	14.5	14.4			12.9	11.7	15.7
La	30.4	26.8			57.6	23.0	18.9
Ce	42.1	48.8			86.9	43.7	42.2
Nd	18.7	21.7			40.9	19.6	17.9
Sm	4.04	3.81			6.04	2.72	2.87
Eu	1.08	1.18			1.56	0.90	1.33
Tb	0.50	0.58			0.69	0.49	0.54
Yb	1.80	1.92			1.83	1.74	2.06
Lu	0.26	0.28			0.26	0.28	0.23
K_2O/Na_2O	0.47	0.41	0.21	0.41	0.91	0.45	0.72
K_2O/CaO	2.51	0.59	0.90	0.78	1.78	0.74	3.60
Sr/Y	5.2	4.3	6.0	7.6	4.7	7.1	3.9
Zr/Y	6.1	5.8	5.3	6.8	6.7	7.9	7.4
Nb/Y	0.50	0.44	0.47	0.65	0.56	0.71	0.65
Ti/Zr	30.7	23.4	32.6	26.1	25.8	27.0	29.5
Th/Yb	2.2	1.8			2.6	2.7	2.0
$[La/Yb]_{cn}$	12.1	10.0			22.6	9.5	6.6
$[Tb/Yb]_{cn}$	1.26	1.37			1.71	1.28	1.19
Eu/Eu*	0.99	1.04			1.00	1.02	1.39

Table 3. Major (wt%) and trace element (ppm) analyses of chlorite schists, Bien Venue Formation (b = below detection limit)

Sample	BVM1	BVM2	BVM3	BVM4	BVM5
SiO_2	47.01	53.00	55.35	50.59	56.17
TiO_2	0.89	1.23	1.37	1.19	1.38
Al_2O_3	7.88	10.75	12.07	10.96	12.99
$Fe_2O_3^{total}$	13.06	16.45	17.49	16.32	15.20
MnO	0.24	0.24	0.19	0.20	0.09
MgO	5.49	3.15	2.85	3.55	4.53
CaO	8.67	5.10	2.00	4.45	1.84
Na_2O	1.58	2.91	2.85	2.97	1.89
K_2O	0.09	0.68	0.70	0.16	0.08
P_2O_5	0.10	0.13	0.15	0.12	0.17
H_2O-	0.07	0.14	0.27	0.04	0.19
H_2O+	1.91	1.64	2.47	1.94	3.45
CO_2	12.85	3.60	1.49	6.39	1.45
Total	99.84	99.02	99.25	98.88	99.43
Ba	192	188	223	215	67
Rb	11	38	27	12	13
Sr	224	178	140	98	44
Cs	0.46	5.99		6.85	0.72
Pb	b	5	b	b	5
U	0.44	0.63		0.55	0.89
Th	1.46	2.11		2.16	2.93
Y	16	22	26	21	23
Nb	6	7	10	9	9
Zr	70	100	119	95	130
Hf	1.97	2.73		2.72	3.70
Ta	0.36	0.47		0.48	0.62
Ga	13	18	19	20	18
V	177	181	204	210	160
Cr	66	17	b	7	b
Sc	19.6	17.0		16.3	16.7
Zn	84	135	160	131	135
Cu	169	100	269	321	314
Ni	78	31	25	36	15
Co	43	45		47	41
La	8.3	11.2		10.7	13.8
Ce	19.8	27.7		25.0	35.2
Nd	13.7	18.5		16.2	20.8
Sm	2.93	4.03		3.79	4.37
Eu	1.59	1.79		1.55	1.72
Tb	0.63	0.78		0.76	0.83
Yb	1.93	2.32		2.27	2.62
Lu	0.32	0.38		0.35	0.42
Ti/V	30	41	40	34	52
Zr/Y	4.4	4.5	4.6	4.5	5.7
Nb/Y	0.38	0.32	0.38	0.43	0.39
Ti/Zr	76.2	73.7	69.0	75.1	63.6
Th/Nb	0.24	0.30		0.24	0.33
Th/La	0.18	0.19		0.20	0.21
Th/Yb	0.8	0.9		1.0	1.1
Ta/Yb	0.19	0.20		0.21	0.24
$[La/Yb]_{cn}$	3.1	3.5		3.4	3.8
$[Tb/Yb]_{cn}$	1.48	1.53		1.52	1.44
Eu/Eu*	1.53	1.32		1.19	1.18

Table 4. Major (wt%) and trace element (ppm) analyses of silicic metavolcaniclastic rocks, Theespruit Formation (b = below detection limit; samples G29 and G34 from Glikson, 1976)

Sample	G29	G34	TJ1	VER1	W1	W2	W3
SiO_2	74.34	79.28	76.13	79.02	74.83	76.41	75.52
TiO_2	0.12	0.20	0.17	0.13	0.13	0.13	0.19
Al_2O_3	11.73	12.60	12.69	12.25	12.49	12.74	12.99
$Fe_2O_3^{total}$	3.64	0.39	1.98	1.02	1.90	1.83	1.94
MnO	0.03	b	0.04	0.01	0.03	0.04	0.02
MgO	3.06	0.85	0.60	0.30	0.23	0.16	0.58
CaO	0.13	0.11	1.05	0.47	0.69	0.66	1.05
Na_2O	3.27	0.11	4.08	3.45	1.91	1.92	2.36
K_2O	0.55	4.01	2.22	4.00	5.96	5.89	3.32
P_2O_5	0.06	0.03	0.04	0.01	0.02	0.02	0.03
LOI	2.81	1.98	1.47	0.42	0.38	0.50	0.73
Total	99.74	99.56	100.47	101.08	98.57	100.30	98.73
Ba	170	1300	752	666	847	733	1014
Rb	24	141	83	70	125	124	79
Sr	22	12	93	57	62	61	11
Cs	0.19	0.46	0.74	0.35			0.53
Pb			15	7	14	13	15
U	3.2	1.5	4.85	3.49			3.16
Th	14	18	21.7	23.1			22.8
Y	27	11	26	16	26	18	21
Nb	23	26	26	22	19	19	20
Zr	280	170	183	144	164	169	173
Hf	5.3	4.4	5.32	4.91			5.53
Ta			1.87	1.87			1.57
Ga			20	18	20	20	20
V	14	13	15	12	11	11	19
Cr	11	14	27	27	31	26	26
Sc	7	6	1.37	0.80			1.55
Zn	62	13	41	16	25	32	25
Cu	108	3	8	14	11	14	9
Ni	39	4	11	10	10	10	9
Co	13	3	2.26	1.27			2.41
La	88	12	72.5	22.1			62.0
Ce	97	29	128	46.4			122
Nd	44	7	43.5	11.9			33.7
Sm	6.4	1.7	6.83	2.19			5.24
Eu	0.84	0.49	0.99	0.43			0.84
Tb	0.55	0.27	0.77	0.44			0.66
Yb	1.9	1.2	2.59	2.12			2.68
Lu			0.40	0.27			0.31
K_2O/Na_2O	0.17	36.5	0.54	1.16	3.12	3.07	1.41
K_2O/CaO	4.23	36.5	2.11	8.51	8.64	8.92	3.16
Sr/Y	0.81	1.09	3.58	3.56	2.38	3.39	0.52
Zr/Y	10.4	15.5	7.0	9.0	6.3	9.4	8.2
Nb/Y	0.85	2.36	1.00	1.38	0.73	1.06	0.95
Ti/Zr	2.6	7.0	5.6	5.4	4.8	4.6	6.6
Th/Yb	7.4	15.0	8.4	10.9			8.5
$[La/Yb]_{cn}$	33.2	7.2	20.1	7.5			16.6
$[Tb/Yb]_{cn}$	1.32	1.02	1.35	0.94			1.12
Eu/Eu*	0.58	0.94	0.56	0.57			0.59

Table 5. Major (wt%) and trace element (ppm) analyses of dacitic metavolcaniclastic rocks, Schoongezicht Formation, Fig Tree Group (b = below detection limit)

Sample	EZ1	EZ2	CON1	SCH5	SCH6	SCH7
SiO_2	63.21	61.67	64.88	62.85	62.15	68.67
TiO_2	0.51	0.59	0.64	0.66	0.74	0.50
Al_2O_3	14.16	14.33	14.89	12.85	14.10	15.40
$Fe_2O_3^{total}$	5.24	5.97	4.18	5.09	5.98	1.78
MnO	0.12	0.09	0.04	0.08	0.09	0.05
MgO	3.28	3.67	3.52	3.12	1.82	0.71
CaO	3.23	3.71	2.09	2.86	2.33	0.88
Na_2O	4.65	4.32	3.91	3.89	2.66	2.23
K_2O	2.94	3.03	3.52	3.64	5.39	6.97
P_2O_5	0.41	0.47	0.33	0.35	0.43	0.13
H_2O-	0.02	0.04	0.04	0.15	0.07	0.06
H_2O+	0.41	0.27	0.45	1.29	1.35	0.64
CO_2	2.00	1.44	0.15	1.78	2.36	1.12
Total	100.18	99.60	98.64	98.61	99.47	99.14
Ba	1057	1045	1243	923	846	893
Rb	94	89	88	113	113	125
Sr	676	578	936	749	302	389
Cs	3.34		3.26	2.18		3.84
Pb	19	30	10	13	b	12
U	2.92		2.72	2.15		1.83
Th	13.2		11.5	7.26		6.24
Y	29	37	27	24	28	15
Nb	8	11	11	10	10	7
Zr	229	240	231	223	226	101
Hf	5.49		5.25	3.56		2.55
Ta	0.51		0.54	0.54		0.34
Ga	25	22	19	17	19	17
V	92	145	84	106	109	46
Cr	70	99	58	115	122	189
Sc	9.34		8.91	2.88		5.76
Zn	88	101	57	92	39	20
Cu	50	41	37	b	21	b
Ni	43	31	25	41	104	67
Co	17.7		12.9	6.22		9.95
La	71.2		53.7	37.1		37.4
Ce	164		114	72.3		71.0
Nd	70.3		53.6	29.4		33.3
Sm	14.3		10.5	4.82		6.43
Eu	3.85		3.49	1.54		2.67
Tb	1.25		1.09	0.46		0.68
Yb	2.12		1.81	0.79		1.30
Lu	0.31		0.18	0.14		0.13
K_2O/Na_2O	0.63	0.70	0.90	0.94	2.03	3.13
K_2O/CaO	0.91	0.82	1.68	1.27	2.31	7.92
Sr/Y	23.3	15.6	34.7	31.2	10.8	25.9
Zr/Y	7.9	6.5	8.6	9.3	8.1	6.7
Nb/Y	0.28	0.30	0.41	0.42	0.36	0.47
Ti/Zr	13.3	14.7	16.6	17.7	19.6	29.7
Th/Yb	6.2		6.4	9.2		4.8
$[La/Yb]_{cn}$	24.1		21.3	33.7		20.6
$[Tb/Yb]_{cn}$	2.68		2.74	2.65		2.38
Eu/Eu*	1.19		1.35	1.35		1.67

Table 6. Geochemical features of barren and VHMS mineralised volcanic suites, Abitibi subprovince, Canada, and comparison with rocks of the Bien Venue Formation

Part A: Abitibi Subprovince, Canada (Barrie et al., 1993)

Group	I		II		III		IV and V	
	Mafic	Felsic	Mafic	Felsic	Mafic	Felsic	Mafic	Felsic
$[La/Yb]_{cn}$	<2	<3.5	2.3-3.6	<3	3-4	3-9	>8	>8
Yb_{cn}	16-50	>40	15-20	20-45	10-15	10-20	2-20	2-25
Zr/Y	<6	<4	<5	<6	<6	<10	>5	>10
Th/Yb	<0.4	<1	0.4-0.6	<0.6	0.6-0.8	0.6-2.5	>1.5	>1
Y (ppm)	>25	>70	20-30	30-60	20-25	15-35	4-40	5-40
Magmatic affinity	Tholeiitic		Transitional tholeiitic - calc-alkaline		Calc-alkaline		Transitional calc-alkaline - alkaline	
Tectono-magmatic setting	Oceanic rift		Rifted island-arc		Continental arc		Arc suites derived from metasomatised mantle with variable crustal contamination	
VHMS deposits	Major VHMS deposits		Major VHMS deposits		Generally barren: only one sulphide deposit known #		Barren	
Example suite	Kamiskotia, Matagami		Noranda, Val d'Or		Selbaie		Upper Skead, Timiskaming	

According to Larson and Hutchinson (1993), most of the Selbaie massive sulphide mineralisation is epigenetic.

Part B: Bien Venue Formation (this study)

Group	III	III / IV	III
Rock type	Quartz-muscovite schist	Biotite-plagioclase schist	Chlorite schist
$[La/Yb]_{cn}$	6.8-12	6.6-23	3.1-3.8
Yb_{cn}	7.1-21	10-12	11-15
Zr/Y	4.0-9.3	5.3-7.9	4.4-5.7
Th/Yb	1.4-3.0	1.8-2.7	0.8-1.1
Y (ppm)	19-39	14-18	16-26
Magmatic affinity	Calc-alkaline	Calc-alkaline	Transitional tholeiitic - calc-alkaline